Journal of Oceanography (2018) 74:115–145
https://doi.org/10.1007/s10872-017-0461-x

REVIEW

Fifty years of the 137°E repeat hydrographic section in the western North Pacific Ocean

Eitarou Oka[1] · Masao Ishii[2,3] · Toshiya Nakano[2,3] · Toshio Suga[4,5] · Shinya Kouketsu[5] · Masatoshi Miyamoto[1] · Hideyuki Nakano[3] · Bo Qiu[6] · Shusaku Sugimoto[7] · Yusuke Takatani[2]

Received: 2 November 2017 / Revised: 25 December 2017 / Accepted: 29 December 2017 / Published online: 23 January 2018

Abstract

The 137°E repeat hydrographic section of the Japan Meteorological Agency across the western North Pacific was initiated in 1967 as part of the Cooperative Study of the Kuroshio and Adjacent Regions and has been continued biannually in winter and summer. The publicly available data from the section have been widely used to reveal seasonal to decadal variations and long-term changes of currents and water masses, biogeochemical and biological properties, and marine pollutants in relation to climate variability such as the El Niño-Southern Oscillation and the Pacific Decadal Oscillation. In commemoration of the 50th anniversary in 2016, this review summarizes the history and scientific achievements of the 137°E section during 1967–2016. Through the publication of more than 100 papers over this 50-year span, with the frequency and significance of the publication increasing in time, the 137°E section has demonstrated its importance for future investigations of physical–biogeochemical–biological interactions on various spatiotemporal scales, and thereby its utility in enhancing process understanding to aid projections of the impact of future climate change on ocean resources and ecosystems over the twenty-first century.

Keywords 137°E section · Western North Pacific · Repeat hydrography · Physical oceanography · Biogeochemical oceanography · Biological oceanography · Marine pollution · Seasonal to decadal variability · Long-term change

1 Introduction

Growing emissions of anthropogenic carbon dioxide (CO_2) and other greenhouse gases are causing warming, acidification, and deoxygenation of the ocean globally (IPCC 2013). To understand the physical and biogeochemical changes and variations in the ocean as well as their controlling mechanisms and impacts/feedbacks on climate and ecosystems, it is imperative that the oceanographic community continues observing the ocean for a prolonged period of time through multidisciplinary approaches. The 137°E repeat hydrographic section, which has been maintained by the Japan Meteorological Agency (JMA), marked its 50th anniversary in 2016. It traverses the Kuroshio, the subtropics, and the tropics in the western North Pacific between Japan and New Guinea (Fig. 1). There are other long-term time series stations and lines such as Station P/Line P in the eastern subarctic North Pacific (Whitney and Freeland 1999), the Hawaii Ocean Time-series program in the central subtropical North Pacific (Karl and Lukas 1996), and the Bermuda Atlantic Time-series Study in the western subtropical North

Electronic supplementary material The online version of this article (https://doi.org/10.1007/s10872-017-0461-x) contains supplementary material, which is available to authorized users.

✉ Eitarou Oka
eoka@aori.u-tokyo.ac.jp

1 Atmosphere and Ocean Research Institute, The University of Tokyo, Kashiwa 277-8564, Japan

2 Global Environment and Marine Department, Japan Meteorological Agency, Tokyo 100-8122, Japan

3 Oceanography and Geochemistry Research Department, Meteorological Research Institute, Tsukuba 305-0052, Japan

4 Department of Geophysics, Graduate School of Science, Tohoku University, Sendai 980-8578, Japan

5 Research and Development Center for Global Change, Japan Agency for Marine-Earth Science and Technology, Yokosuka 237-0061, Japan

6 Department of Oceanography, University of Hawaii at Manoa, Honolulu, HI 96822, USA

7 Frontier Research Institute for Interdisciplinary Sciences, Tohoku University, Sendai 980-8578, Japan

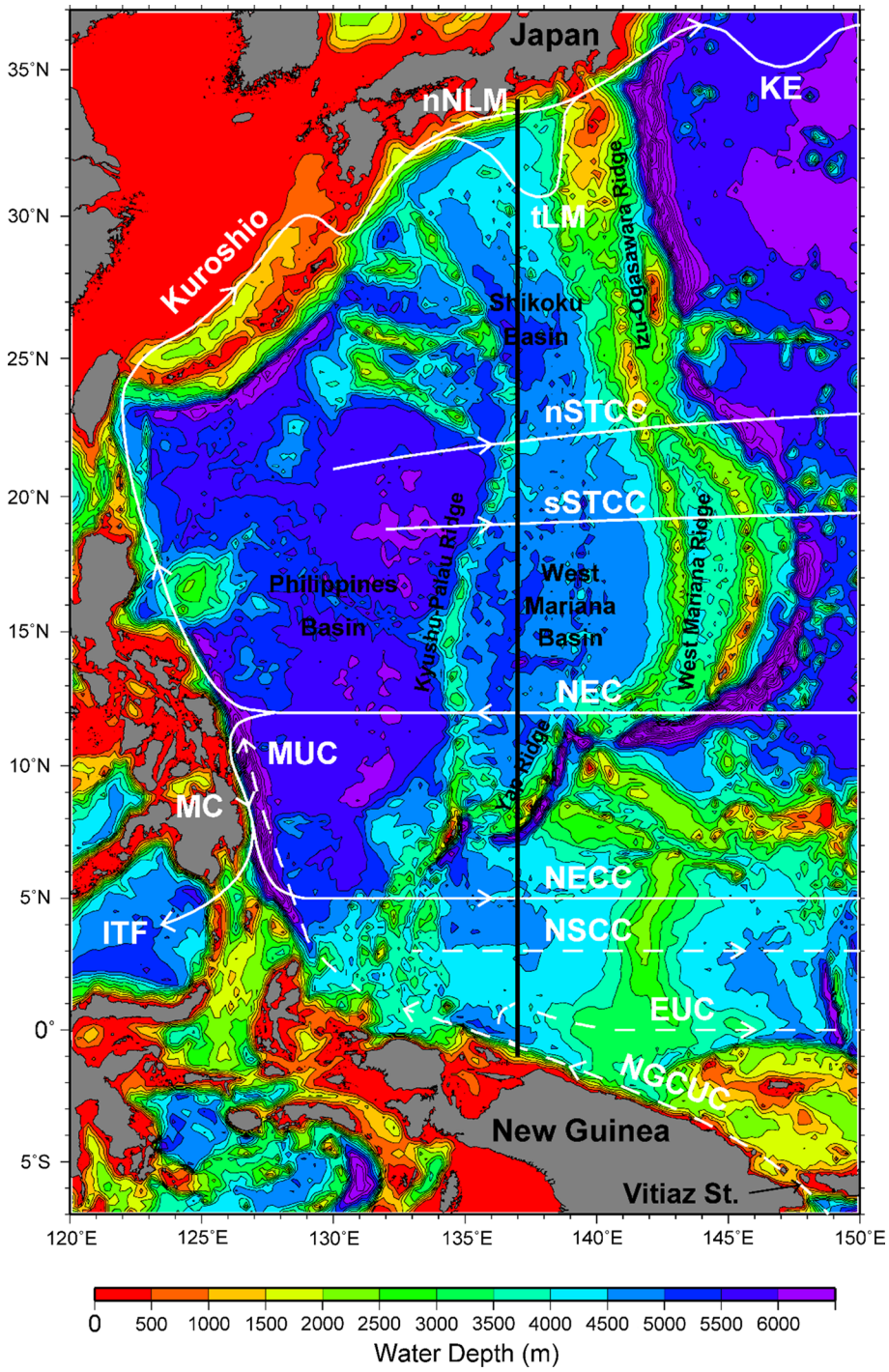

Fig. 1 The 137°E section (thick black line) and the associated surface and subsurface currents (solid and dashed white lines). KE Kuroshio extension, nSTCC (sSTCC) northern (southern) STCC (Kobashi et al. 2006), NEC North equatorial current, MC Mindanao current, MUC Mindanao undercurrent, ITF Indonesian through flow, NECC North Equatorial Countercurrent, NSCC North Subsurface Countercurrent, EUC Equatorial Undercurrent, NGCUC New Guinea Coastal Undercurrent. nNLM and tLM denote a nearshore non-large-meander path and a typical large-meander path of the Kuroshio, respectively (Kawabe 1995). Note that the width of currents is not considered, particularly for the NEC (see Fig. 4). Thin black contours with color indicate isobaths at an interval of 500 m, based on ETOPO2v2 (National Geophysical Data Center 2006)

Atlantic (Michaels and Knap 1996). However, none of them is comparable to the 137°E section in terms of the meridional and vertical extent and the variety of measured variables (Bingham et al. 2002).

The 137°E section was initiated in 1967 as part of the Cooperative Study of the Kuroshio and Adjacent Regions (CSK) supported by the Intergovernmental Oceanographic Commission, UNESCO under the leadership of Dr. Jotaro Masuzawa (Photo 1), who was a Senior Scientific Officer of the JMA in 1956–1971 and the Director-General later in 1980–1983 (Masuzawa 1967; Kuroda 2017). Enlightened by Prof. Raymond B. Montgomery during his stay at the Johns Hopkins University in 1962–1964 (Masuzawa and Nagasaka 1975), Masuzawa aimed to "establish an observational framework for ocean monitoring, at least in the western North Pacific as the Japanese area of responsibility", "in order to investigate common variability in phenomena on as large a scale as possible" (Masuzawa 1978). Impressively,

Photo 1 Dr. Jotaro Masuzawa (1922–2000) (after Nakano 2016)

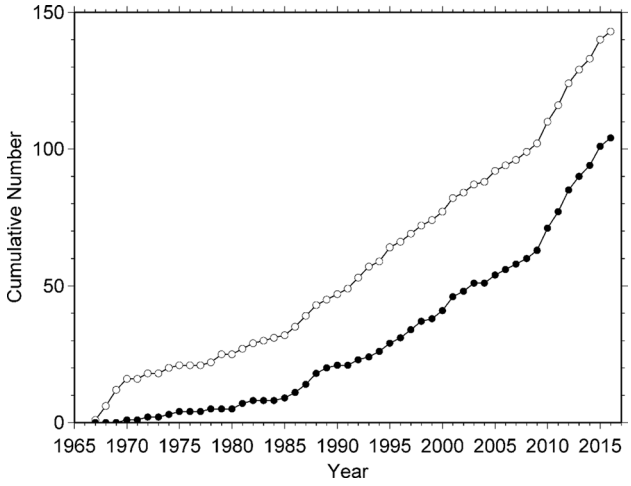

Fig. 2 Cumulative number of papers using the 137°E section data published in all journals and books (Supplementary Table S1; circles) and those excluding three in-house journals of the JMA (*Geophysical Magazine, Oceanographical Magazine*, and *Weather Service Bulletin*; dots), plotted against year from 1967 through 2016

his foresight and vocation emerged long before the 1980s, during which time the world shared the recognition that it is of crucial existential importance for human society to accurately understand the changes in the ocean that play an essential role in regulating climate and ecosystems, followed by the establishment of the Global Ocean Observing System in 1991. Masuzawa chose the 137°E meridian "to observe major currents and water masses as undisturbed by islands and submarine mountains as possible" (Mazuzawa 1967; Fig. 1). It is worth noting that at that time the research community had not identified or described some of the major currents/water masses appearing in the 137°E section, such as the Subtropical Countercurrent (STCC; Uda and Hasunuma 1969), the Subtropical Mode Water (STMW; Masuzawa 1969), and the North Subsurface Countercurrent (NSCC; Tsuchiya 1975). In addition, while global warming as a result of anthropogenic CO_2 emission and its partial absorption by the ocean had been surmised (Revelle and Suess 1957), the impact of the resultant carbonate system changes in seawater on marine ecosystems as well as the decline of dissolved oxygen (O_2) had not been recognized.

The first historical survey of the 137°E section was conducted in January 12–24, 1967 over a distance of 3860 km between 34°N and 0°45′S in the first cruise of R/V Ryofu-maru II (Mazuzawa 1967). Since then, the observational program has not been interrupted for more than 50 years, in particular during the earlier period when little scientific achievement was made (Fig. 2). A decade after the launch, Masuzawa (1978) expressed his concern: "There has been always a doubt in my mind about what we can reveal from yearly observations, even for examining large-scale, long-term variations." "Although the section has weathered hardships for more than 10 years, my concern that it can be all pain and no gain has not gone away. While I secretly have an irreverent idea that the value of the section should be judged in 30 years, the responsibility of planning still weighs heavily on my shoulders." Despite his doubt, more than 100 papers using the 137°E data have been published during the past 50 years (Supplementary Table S1) with increasing frequency (Fig. 2) and with increasing significance. Among them, seven (Midorikawa et al. 2005, 2010; Nakano et al. 2007; Ren and Riser 2010; Ishii et al. 2011; Purkey and Johnson 2012; Qiu and Chen 2012) were quoted by Chapter 3 of the Intergovernmental Panel on Climate Change (IPCC) Fifth Assessment Report on ocean observation (Rhein et al. 2013). For the half-century-long contributions to the advancement of marine science through monitoring and data management, the 9th POMA Award was given from the North Pacific Marine Science Organization (PICES) to the 137°E section in 2016.

In this review, we summarize scientific achievements accomplished through analyses of the 137°E data. In addition to these studies, many others have used the data in combination with other observations for various targets, e.g., to investigate surface thermohaline variability in the tropical Pacific (Ando and McPhaden 1997), to estimate global air–sea fluxes of CO_2 (Takahashi et al. 1997 and its updates), and to calculate nitrate transport by the Kuroshio from the East China Sea to the south of the Kuroshio (Guo et al. 2013). Modelling studies have also used the 137°E data for initial conditions and for validations, particularly in recent years (e.g., Luo and Yamagata 2003; Fujii et al. 2009; Shibano et al. 2011; Wada et al. 2011; Yara et al. 2012; Qiu et al. 2014b; Nishikawa et al. 2015; Chen et al. 2016; Tseng et al. 2016; Toyoda et al. 2017).

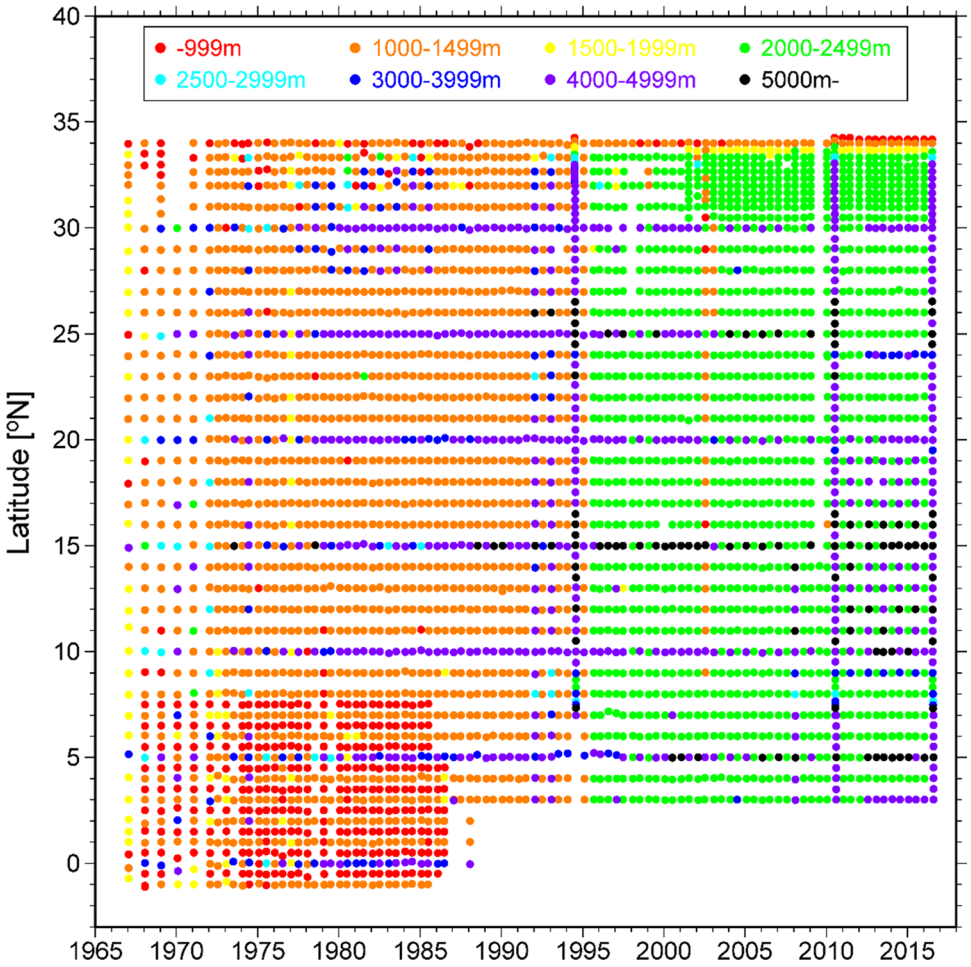

Fig. 3 Latitude of hydrographic observations in winter and summer at the 137°E section, plotted against year from 1967 through 2016. The color of dots indicates the maximum depth of standard layers at each station

Section 2 introduces the observation history of the 137°E section. Section 3 describes the typical distribution of currents and water masses in the 137°E section. Sections 4 and 5 present scientific achievements in physical and biogeochemical oceanography, respectively. Section 6 demonstrates achievements in the other research fields—specifically, in terms of biological properties and marine pollution. Section 7 summarizes the achievements from the 137°E section, evaluates the extent to which Dr. Masuzawa's aims were attained, and discusses implications for future research and directions.

2 Observation history

In the earlier years, the 137°E section was visited from 34°N to 1°S in the latter half of January (the time period and southward progression of winter observations have been unchanged for 50 years) with a typical station interval of 40′ north of 32°N, 1° at 8°N–32°N, and 30′ south of 8°N (Masuzawa 1967, 1968; Akamatsu and Sawara 1969; Masuzawa et al. 1970; Nagasaka and Sawara 1972; Shuto 1996; Fig. 3). At each station, temperature (T) was measured using reversing thermometers and water samples were collected by Nansen bottles (Photo 2) down to 1250 m depth, except for 4000 m at every 5° between 30°N and the equator. Depth was determined by wire angle at depths less than 100 m and by the thermometric method using a pair of pressure-protected and unprotected thermometers at depths greater than 100 m. Water samples were analyzed for a wide variety of parameters, such as salinity (S), O_2, nutrients (Masuzawa et al. 1970; Sagi 1970), ammonia (Sagi 1969b), pH and total alkalinity (Akiyama et al. 1968), calcium (Sagi 1969a), trace metals such as iron and manganese, chlorophyll-a and pheophytin (Kawarada and Sano 1969), phytoplankton and zooplankton (Kawarada et al. 1968), among others. In the equatorial region, current velocity from the surface to 500 m depth relative to 600–900 m was measured by two TS-II (Roberts-type) current meters from the drifting vessel to supplement geostrophic calculations (Bessho 1995). Maritime meteorological observations were also carried out routinely, eight times a day (Hayashi et al. 1968, 1970).

Photo 2 Water sampling from Nansen bottles and reading reversing thermometers onboard R/V Ryofu-maru II (around 1969) (Japan Meteorological Agency, personal communication)

In 1972, in response to the domestic enforcement of the Act on Prevention of Marine Pollution and Maritime Disaster in the previous year, the JMA started the Observation for Monitoring Background Marine Pollution targeting heavy metals (mercury and cadmium), and made the 137°E section biannual by adding summer observations around July[1] (Sagi et al. 1974; Kamiya 2013; Fig. 3). The observations south of 3°N had been continued until summer 1986, but were discontinued in summer 1988; subsequently, the 137°E section has been occupied between 3°N and 34°N. A conductivity–temperature–depth profiler (CTD) mounted with Niskin bottles and a bottom-mounted acoustic Doppler current profiler (ADCP) were introduced in summer 1988, enabling high-resolution profiling of *T* and *S* with respect to pressure, water sampling at precise depths, and measurements of subsurface current velocity (Shuto 1996).

[1] The Observation for Monitoring Background Marine Pollution was launched not only at the 137°E section but also at a meridional section along 165°E and five sections around Japan (PH, PK, PM, PN, and PT). The five sections were named after the combination of the initial of "Pollution" and that of the four Marine Observatories of JMA (Hakodate, Kobe, Maizuru, and Nagasaki) and the headquarters in Tokyo (Ogawa and Takatani 1998).

As a number of the hydrographic sections of the JMA in the western North Pacific were selected as the repeat sections of the World Ocean Circulation Experiment Hydrographic Program (WHP) during 1990–1994, the JMA further improved its observation skill while coordinating these sections and carried out the 137°E section in summer 1994 as the WHP P9 one-time section, which was characterized by full-depth, high-resolution, and multi-parameter observations (Kaneko 1998; Kaneko et al. 1998). The standard observation depth of the regular 137°E section extended down to 2000 m in summer 1995 in conjunction with the launch of R/V Ryofu-maru III (Kaneko 2002; Fig. 3). The observations in the Kuroshio region were further augmented in summer 2001, resulting in the present station interval of 20′ north of 31°N, 30′ at 30°N–31°N, and 1° south of 30°N. In addition to the winter and summer observations shown in Fig. 3, those in spring and fall were conducted between 1992 and 2009 (e.g., Qiu and Chen 2010a, 2012), although the observations by R/V Keifu-maru I before 2001 had some shortcomings, such as lower-quality *S* data, larger station spacing, and smaller observational depth range.

To develop a globally coordinated network of sustained hydrographic sections after the completion of WHP, the Global Ocean Ship-based Hydrographic Investigations Panel (GO-SHIP), which is now part of the Global Climate Observing System and the Global Ocean Observing System, was established in 2007 with distinguished coordinating services by the International Ocean Carbon Coordination Project and the Climate Variability and Predictability Program (CLIVAR) (Hood et al. 2009). After conforming to the higher data quality standard of GO-SHIP, the JMA launched high-accuracy hydrographic observations by R/Vs Ryofu-maru III and Keifu-maru II in spring 2010, and conducted P9 revisit observations in summer 2010 and summer 2016 (Kamiya 2013) covering all the level-1 variables of GO-SHIP (http://www.go-ship.org/DatReq.html). In the regular 137°E section cruises with longer station intervals and limited sampling depths, most of the level-1 variables including many of Essential Ocean Variables for physics and biogeochemistry (http://www.goosocean.org/) have been measured. Since summer 2010, dissolved O_2 profiles have been collected continuously by a rapid-response optical sensor RINKO-III (JFE Advantech Co., Ltd.) mounted on the CTD and reported after calibrating with the dissolved O_2 data from the Winkler titration method (Uchida et al. 2011; Sasano et al. 2011).

The data obtained by shipboard observations of the JMA, including measurements along the 137°E section, are publicly available online (http://www.data.jma.go.jp/gmd/kaiyou/db/vessel_obs/data-report/html/ship/ship_e.php). These include the cruise summary, the station information, and data of hydrography, CTD and expendable CTD, expendable and digital bathythermograph, water sampling,

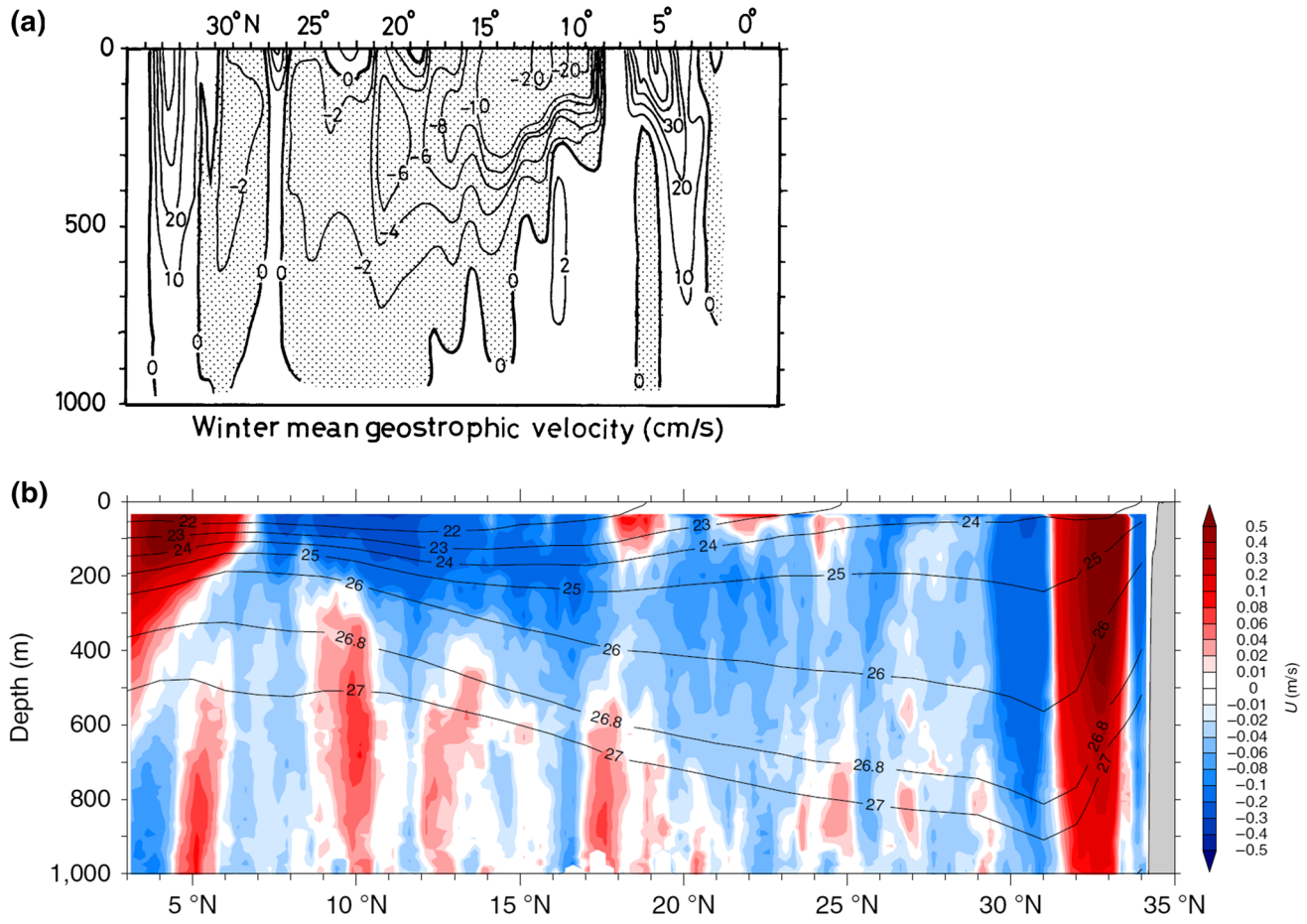

Fig. 4 **a** Distribution of eastward geostrophic velocity (cm s^{-1}) relative to 1000 dbar in the winter 137°E section, averaged between 1967 and 1987. Number on the ordinate denotes depth in meters. Negative values are hatched (after Shuto 1996). **b** Distribution of eastward velocity measured by ADCP (color) and potential density (kg m^{-3}) obtained by CTD (black contours) in the 137°E section, averaged between 2004 and 2016 (after Qiu et al. 2017)

greenhouse gases, petroleum hydrocarbon and heavy metals, floating pollutants, tar ball, maritime meteorology, and aerology. Among these data sets, those from cruises that meet GO-SHIP criteria have been submitted to the CLIVAR and Carbon Hydrographic Data Office (https://cchdo.ucsd.edu/). All datasets from cruises with ocean interior high-precision carbonate system measurements (Sect. 5) have also been stored in the Pacific Ocean Interior Carbon Database (PACIFICA; Suzuki et al. 2013; https://www.nodc.noaa.gov/ocads/oceans/PACIFICA/) and the Global Ocean Data Analysis Project Version 2 (GLODAPv2; Olsen et al. 2016; https://www.nodc.noaa.gov/ocads/oceans/GLODAPv2/). Data of underway CO_2 measurements in surface seawater since the early 1980s (Sect. 5) have also been available in the Global Surface pCO_2 (LDEO) database (Takahashi and Sutherland 2017; https://www.nodc.noaa.gov/ocads/oceans/LDEO_Underway_Database/) and the Surface Ocean CO_2 Atlas (SOCAT; Bakker et al. 2016; https://www.socat.info/).

3 Typical distribution of currents and water masses in the 137°E section

The 137°E section crosses the western part of the North Pacific subtropical gyre and the North and South Pacific tropical gyres, and numerous zonal currents that are components of these gyres (Fig. 1). The Kuroshio, which is the western boundary current of the North Pacific subtropical gyre, usually flows eastward at 33°N along the southern coast of Japan (Fig. 4), but frequently shifted offshore as far south as 30°N forming a large-meander path from the mid-1970s to the early 1990s (Qiu and Joyce 1992; Kawabe 1995; horizontal bars at the bottom of each panel in Fig. 8). To the south of the Kuroshio exists weak westward flow associated with the recirculation gyre of the Kuroshio, which has been often called the Kuroshio Countercurrent. Farther south, the North Equatorial Current (NEC) flows westward broadly between 25° and 7°N. Its northern part north of 15°N reaches a depth of 1000 m with a subsurface current

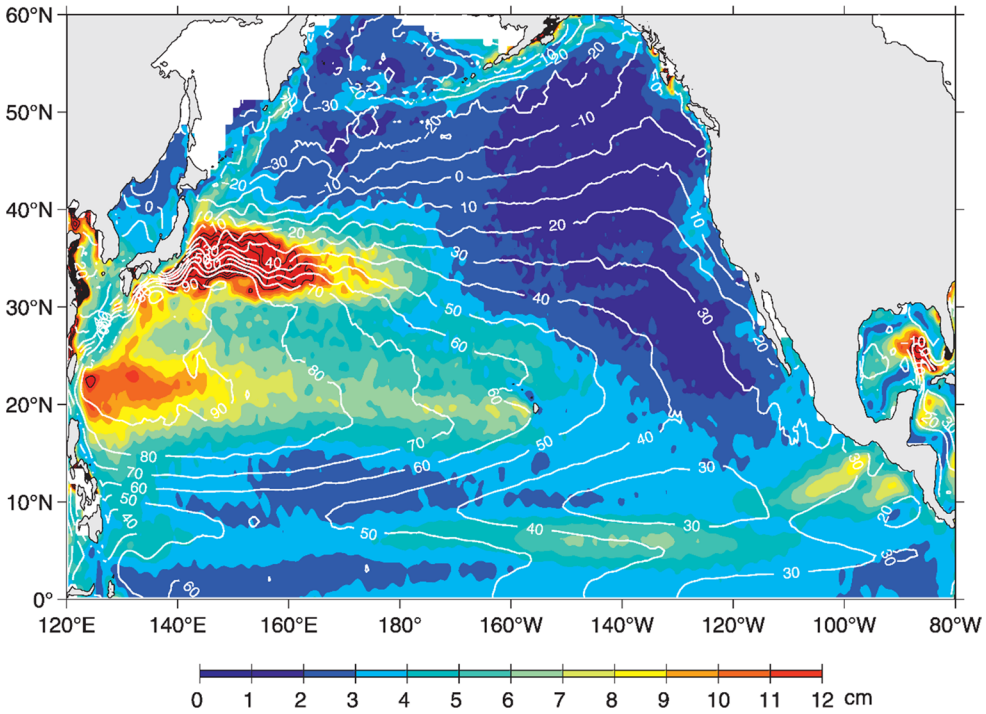

Fig. 5 Root-mean-squared sea surface height variability in the North Pacific based on high-pass-filtered satellite altimeter data from October 1992 to April 2009. Regions where the variability exceeds 12 cm are indicated by thin black contours. White contours denote the mean sea surface height field (cm) by Niiler et al. (2003) (after Qiu and Chen 2010a). © Copyright 2010 American Meteorological Society (AMS). Permission to use figures, tables, and brief excerpts from this work in scientific and educational works is hereby granted provided that the source is acknowledged. Any use of material in this work that is determined to be "fair use" under Section 107 of the U.S. Copyright Act or that satisfies the conditions specified in Section 108 of the U.S. Copyright Act (17 USC §108) does not require the AMS's permission. Republication, systematic reproduction, posting in electronic form, such as on a website or in a searchable database, or other uses of this material, except as exempted by the above statement, requires written permission or a license from the AMS. All AMS journals and monograph publications are registered with the Copyright Clearance Center (http://www.copyright.com). Questions about permission to use materials for which AMS holds the copyright can also be directed to the AMS Permissions Officer at permissions@ametsoc.org. Additional details are provided in the AMS Copyright Policy statement, available on the AMS website (http://www.ametsoc.org/CopyrightInformation)

core at 200–300 m, while the southern part south of 15°N has a thickness of 300–500 m and is strongest at the surface (Masuzawa 1967). Embedded in the northern NEC between 18°N and 24°N, multiple subtropical fronts and the associated STCCs flow eastward in the shallow layer (Masuzawa 1967; Kimura 1982), corresponding to the northward shoaling of isotherms in the upper 200 m in contrast with the northward deepening in the underlying layers (Fig. 7a). As a result of the baroclinic instability associated with the reversal of the current direction between the STCC and the NEC, the STCC region exhibits large mesoscale eddy variability, being second only to the Kuroshio Extension region in the North Pacific (Qiu 1999; Fig. 5). At 2°N–7°N, the North Equatorial Countercurrent (NECC) flows eastward in the shallow layer above the thermocline (at ~ 200 m; Fig. 4). Its core shifts southward with increasing depth and connects to that of the eastward-flowing NSCC in the subthermocline layers on the long-term average (Qiu and Joyce 1992; Gouriou and Toole 1993), while the two cores are observed separately in some individual sections (Guan 1986; Bingham and Lukas 1995; Fig. 6).

Underneath the NEC and the NECC, the recently identified North Equatorial Undercurrents (NEUCs; Qiu et al. 2013a) flow eastward at depths greater than 300 dbar at 5°N, 9°N, 13°N, and 18°N (Fig. 4b). The existence of quasi-stationary NEUCs across the tropical North Pacific was first suggested by geostrophic velocity distributions in the 137°E section referred to 2000 dbar after 1995 (Fig. 3) that, unlike those referred to shallower depths before 1995 (e.g., Fig. 4a; Qiu and Joyce 1992), captured these jets in the intermediate layer (Bo Qiu, personal communication). It was then confirmed (Qiu et al. 2013a) by the subsurface velocity distribution in the North Pacific based on *T*/*S* measurements by Argo profiling floats (Roemmich et al. 2001). The NEUCs may be a part of quasi-zonal jet-like structures, which are ubiquitous over the global ocean (e.g., Maximenko et al. 2005) and whose formation mechanism has been actively investigated (see Chen et al. 2015 for reviews and extensive

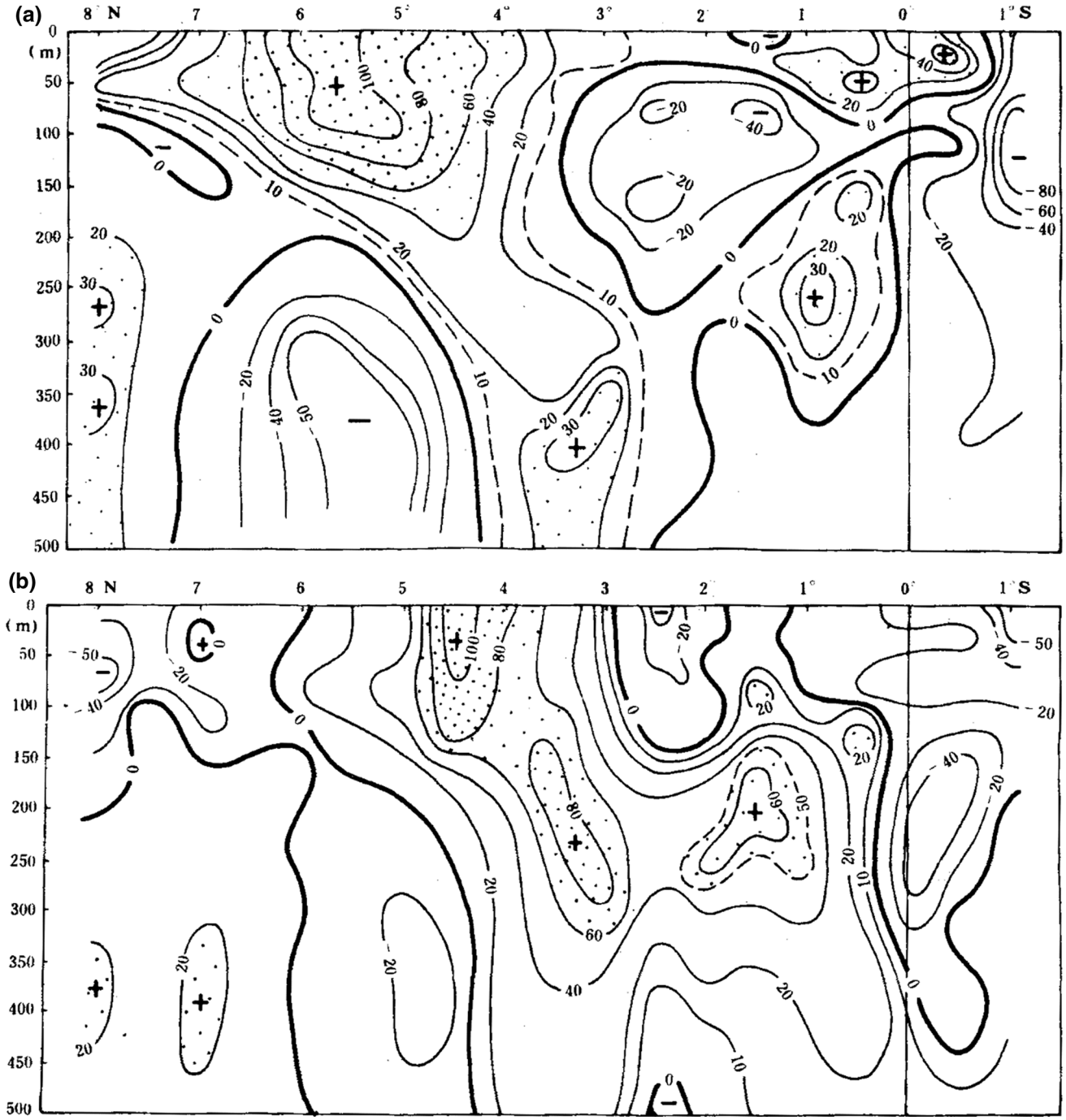

Fig. 6 Distributions of eastward velocity (cm s^{-1}) measured by two current meters in the 137°E section in **a** winter and **b** summer of 1981 (after Guan 1986)

references). Based on analyses of an eddy-resolving ocean general circulation model and a 1.5-layer reduced gravity model, the companion paper (Qiu et al. 2013b) also offered a formation mechanism; the NEUCs are formed by breaking of wind-forced baroclinic Rossby waves, which are generated annually at the eastern boundary of Pacific basin, due to nonlinear triad interactions, and the subsequent eddy–eddy interactions.

In the equatorial region, direct current measurements by two current meters until 1986 (Sect. 2) yielded a consistent structure (Masuzawa 1967, 1968, 1970; Akamatsu and Sawara 1969; Nagasaka and Sawara 1972; Guan 1986;

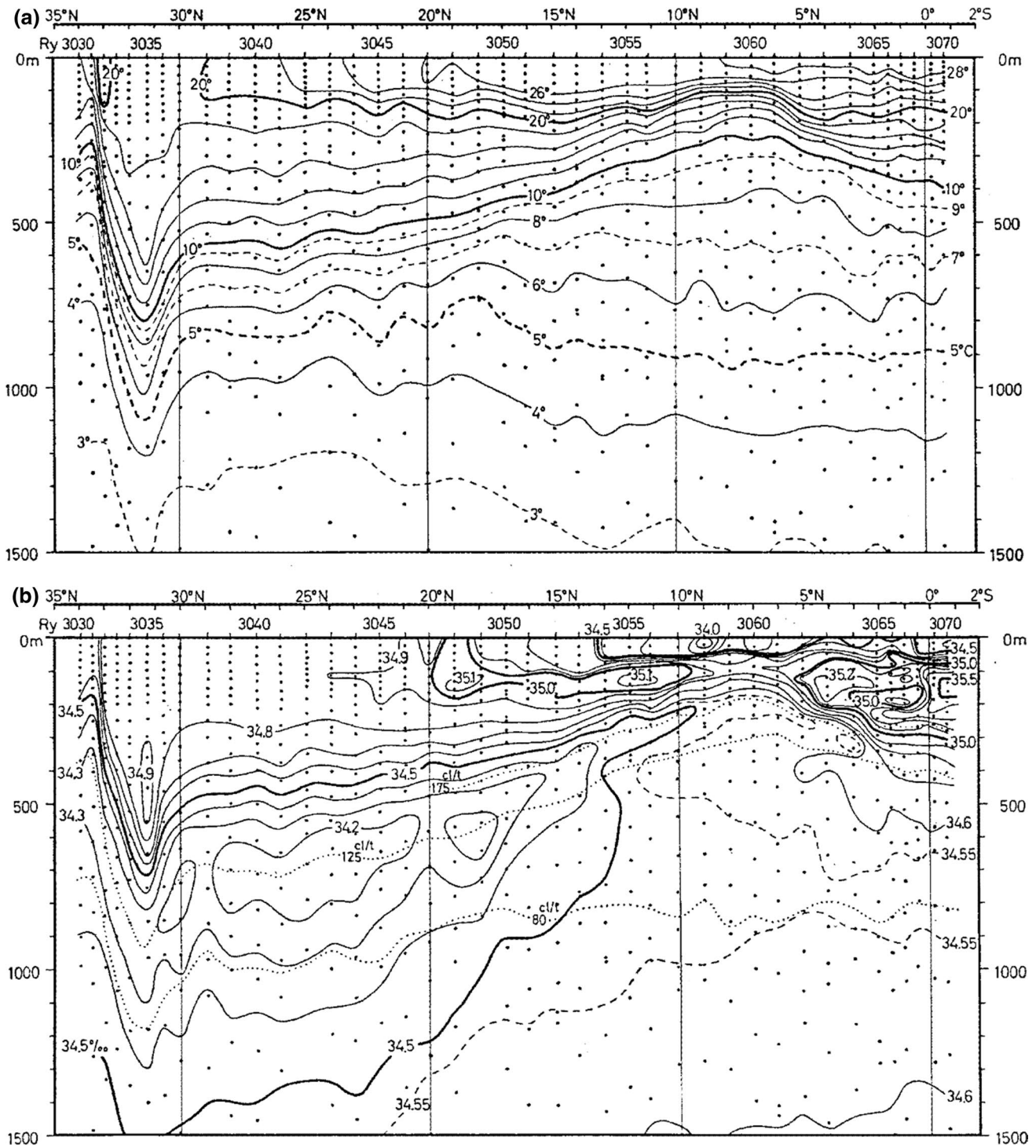

Fig. 7 Distributions of **a** T and **b** S in the 137°E section in winter 1967. Dots indicate the observation locations. Dotted lines in **b** indicate thermosteric anomaly contours of 175, 125, and 80 centiliters per ton (cl/t), which correspond to σ_t = 26.26, 26.79, and 27.26 kg m^{-3} (σ_t is potential density calculated using T instead of θ) (after Masuzawa 1967)

Bingham and Lukas 1995; Fig. 6). The eastward-flowing Equatorial Undercurrent (EUC; Cromwell et al. 1954), which begins north of New Guinea and appears as a strong subsurface jet on the equator in the central to eastern Pacific (e.g., Wyrtki and Kilonsky 1984), is observed as a relatively weak jet at 100–300 m, 0.5°N–1.5°N in the 137°E section. Between the equator and 1°S, the monsoonal New Guinea Coastal Current (NGCC; Wyrtki 1961) flows eastward in

boreal winter and westward in boreal summer along the northern coast of New Guinea at the surface, while the New Guinea Coastal Undercurrent (NGCUC; Lindstrom et al. 1987; Tsuchiya et al. 1989), which is the low-latitude western boundary current of the tropical South Pacific, flows westward at depths greater than 100 m throughout the year. A majority portion of the NGCUC turns east near and east of the 137°E section to feed the EUC (Tshuchiya et al. 1989; Gouriou and Toole 1993; Bingham and Lukas 1995), and some of the remaining portion turns east in the downstream regions to feed the NSCC and the NECC (Tsuchiya 1991; Talley et al. 2011).

These currents transport various water masses originating from the North and South Pacific to the 137°E section (Fig. 7). The subsurface S maximum centered at 150 m, 15°N is the North Pacific Tropical Water (NPTW; Cannon 1966; Tsuchiya 1968), also referred to as the North Pacific Subtropical Underwater. NPTW is formed in the central part of the North Pacific subtropical gyre where evaporation dominates precipitation and is transported westward by the NEC. The S minimum at 500–900 m north of 17°N along the isopycnal of $\sigma_\theta = 26.8$ kg m^{-3} (θ is potential temperature and σ_θ is potential density) is the North Pacific Intermediate Water (NPIW; Sverdrup et al. 1942; Reid 1965). NPIW originates in the Okhotsk Sea, enters the North Pacific subtropical gyre through the mixed water region east of Japan, and is then advected westward by the Kuroshio recirculation and the northern NEC (Talley 1993; Yasuda 2004; Fujii et al. 2013). The S minimum in the 137°E section extends southward of 17°N, beyond which its σ_θ decreases from 26.8 to 26.5–26.3 kg m^{-3}. The S minimum at 11°N–17°N at $\sigma_\theta < 26.6$ kg m^{-3} is the Tropical Salinity Minimum (TSM; Yuan and Talley 1992), which is formed in the eastern North Pacific through merging of NPIW and the Shallow Salinity Minimum formed in the California Current region (Reid 1973) and is transported westward by the lower part of the NEC.

The S maximum centered at ~ 150 m, south of 6°N is the South Pacific Tropical Water (Cannon 1966), while the S minimum at ~ 700 m, south of 11°N at $\sigma_\theta = 27.2$ kg m^{-3} is the Antarctic Intermediate Water (Sverdrup et al. 1942; Reid 1965). These waters formed in the South Pacific are transported westward to the eastern coast of Australia by the South Equatorial Current, then northward through the Coral and Solomon Seas by the Great Barrier Reef Undercurrent and the North Queensland Current, and finally northwestward through the Vitiaz Strait (Fig. 1) to the western equatorial Pacific by the NGCUC (Tsuchiya et al. 1989; Tsuchiya 1991; Qu and Lindstrom 2002). Subsequently, the South Pacific Tropical Water is transported eastward by the EUC and the NECC (Masuzawa 1972; Tsuchiya et al. 1989). Some Antarctic Intermediate Water is advected eastward by the NSCC, while most of it is transported northward along the eastern coast of Mindanao by the Mindanao Undercurrent (Tsuchiya 1991; Hu and Cui 1991; Fine et al. 1994).

Another feature seen in the 137°E section is the weak stratification near the top of the thermocline at 16–18 °C south of the Kuroshio (Fig. 7a). This structure was termed STMW by Masuzawa (1969) because it produces a mode in the volume distribution on the T–S diagram for the subtropical gyre. Subsequently, the moniker mode water has been applied to all similar water masses characterized by weak stratification or low potential vorticity (PV) in the world oceans (Hanawa and Talley 2001).

4 Scientific achievements in physical oceanography

The data from the 137°E section are best applied to investigations of temporal variations of the meridional–vertical structures and their integrated values (e.g., dynamic height, cross-sectional area, and volume transport) in relation to climate variations. During the first two decades, they were analyzed to reveal interannual variations of thermohaline structures and currents. This was mainly considered in the tropical region in relation to the El Niño-Southern Oscillation (ENSO) (Masuzawa and Nagasaka 1975; Guan 1986; Andow 1987; Saiki 1987), as well as to typhoon occurrence (Nagasaka 1981), weather in Japan (Kurihara 1984, 1985), and the Indian summer monsoon (Yasunari 1990). The 137°E data were also combined with other meridional transects to demonstrate that the decorrelation length scale of and the necessary sampling density for subsurface temperature variability in the western North Pacific is 3° (lat.)/3° (lon.) at 17.5°N–30°N and 6°/10° at 5°N–17.5°N (White et al. 1982), which rationalized expansion of a regional expendable bathythermograph observation network of the North Pacific Experiment to the entire Pacific in 1980 (White 1995).

Since Hanawa et al. (1988) examined winter mixed layers south of the Kuroshio in relation to ENSO, a number of studies have also used the 137°E data to explore the subtropics. Moreover, extension of the time series has enabled us to describe not only interannual but also decadal variability (Shuto 1996), particularly in relation to the Pacific Decadal Oscillation (PDO; Mantua et al. 1997), and now to separate decadal variability and long-term trends (Qiu and Chen 2012; Oka et al. 2017). In the following part of this section, we review scientific achievements in physical oceanography from the 137°E section, mainly over the last 30 years in terms of thermohaline structures (Sect. 4.1) and large to mesoscale currents (Sect. 4.2). In addition, the 137°E data have contributed to studies on submesoscale and microscale phenomena in recent years (Sect. 4.3). These studies on smaller scales have benefitted from the CTD and

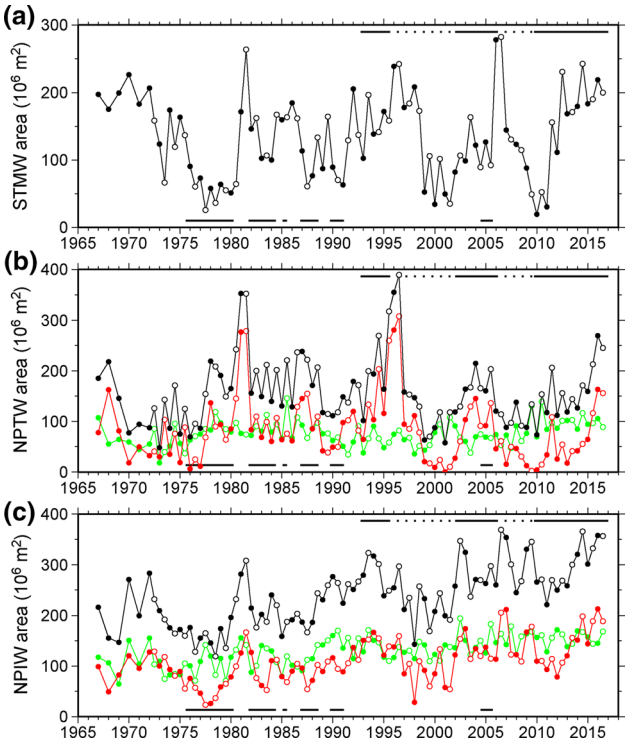

Fig. 8 Time series of cross-sectional area of **a** STMW, **b** NPTW, and **c** NPIW in the 137°E section during 1967–2016, calculated from optimally interpolated *T*/*S* data of Nakano et al. (2007). Here, STMW is defined as regions of PV $< 2.0 \times 10^{-10}$ m^{-1} s^{-1} and $\theta = 16$–19.5 °C (e.g., Suga et al. 1989), NPTW as regions of $S > 34.9$ north of 7°N (e.g., Suga et al. 2000), and NPIW as regions of $S < 34.2$ at depths greater than 200 dbar (e.g., Shuto 1996). Dots (circles) represent winter (summer) observations. Red (green) plots in **b** and **c** indicate the area north (south) of 18°N and 25°N, respectively. Horizontal bars at the bottom of each panel denote large-meander periods of the Kuroshio. Solid (dotted) bars at the top of each panel indicate stable (unstable) periods of the KE after October 1992

ADCP measurements repeated along the section since summer 1988, which have facilitated a reduction in the error bars of estimations and clarified temporal variability of the phenomena.

4.1 Thermohaline structures

After its discovery (Masuzawa 1969), STMW had been left unexplored for two decades, until its formation process associated with deep winter mixed layers south of the Kuroshio and the Kuroshio Extension (KE) was investigated by Hanawa (1987) and Hanawa and Hoshino (1988). Following these studies, Suga et al. (1989) examined STMW in the 137°E section in the winters spanning 1967–1987 and the summers spanning 1972–1986. By using apparent oxygen utilization (AOU), they clarified that a half (1)-year-old STMW appeared in the summer (winter) section as far south as 26°N (23°N), suggesting differences in the formation region and the subsequent southwestward advection by the Kuroshio recirculation that were verified later by using climatological data (Suga and Hanawa 1990, 1995a) and Argo profiling float data (Oka 2009).

As for year-to-year variability, Suga et al. (1989) demonstrated that less STMW was advected from the east during large-meander periods of the Kuroshio (Fig. 8a), during which anomalously warm STMW was formed locally around 137°E, that is, in an isolated recirculation gyre west of the Kuroshio large meander (Hayashi 2008; Sugimoto and Hanawa 2014). Furthermore, Suga and Hanawa (1995b) analyzed the 137°E section up to 1991 to indicate that during non-large-meander periods of the Kuroshio, STMW with lower PV and lower AOU tended to be formed in winters with stronger monsoon expression, suggesting the importance of surface cooling. On the other hand, Soga et al. (2005) examined the summer occupation of the 137°E section up to 2004 to point out that thinner and warmer STMW was formed around 2000 despite moderately strong cooling. Supporting their result, Qiu and Chen (2006) analyzed *T* profiles south of the KE during 1993–2004 to demonstrate that the STMW formation is largely controlled by PDO-related decadal variability of the KE, its southern recirculation gyre, and the associated eddy field[2] (Qiu and Chen 2005; Qiu et al. 2007, 2014a). Specifically, the STMW formation weakens (strengthens) during unstable (stable) periods of the KE (Fig. 8a), likely because high (low) eddy activity transports more (less) high PV water north of the KE to the STMW formation region to hinder (facilitate) deepening of winter mixed layers. Such importance of oceanic control on the STMW formation and subduction was confirmed by analyses of decade-long Argo profiling float data (Rainville et al. 2014; Oka et al. 2015; Cerovečki and Giglio 2016), although it does not preclude or deny the importance of atmospheric control prior to 1991. An analysis of historical *T* profiles over 1968–2014 indicated that the STMW formation was controlled primarily by surface cooling during the late 1970s and 1980s and by oceanic processes after ~ 1990 (Sugimoto and Kako 2016). Furthermore, an analysis of the 137°E section over winters spanning 1967–2016 demonstrated that for the last 25 years, *S* of STMW decreased (increased) during unstable (stable) KE periods, which can be also explained by the decadal variability in water exchange between the saline subtropics and the fresher mixed water region across the KE

[2] The decadal variability of the KE system, which was detected by satellite altimeter measurements initiated in 1992 (Ducet et al. 2000), is driven by PDO-related wind forcing in the central North Pacific. When negative (positive) sea surface height anomalies generated in the warm (cool) phase of PDO reach the area east of Japan after propagating westward for 3–4 years, the KE turns into an unstable (stable) state and is accompanied by a weakened (strengthened) southern recirculation gyre and high (low) regional eddy activity.

(Oka et al. 2017). Interestingly, such decadal S variability of STMW was almost in phase along the 137°E section against our expectation from the climatological STMW circulation (Bingham et al. 2002), suggesting the importance of horizontal eddy mixing.

Studies on low-frequency variability of NPTW based on the 137°E section data have been advanced with the development of other hydrographic data and surface flux data. Shuto (1996) analyzed NPTW in the 137°E section spanning 1967–1987, although its relation to surface freshwater fluxes in the formation region, he mentioned, could not be evaluated because of the absence of evaporation and precipitation data. By using available wind stress data, he demonstrated that on decadal time scales, the cross-sectional area of NPTW ($S > 35.0$) corresponded to the absolute maximum of negative wind stress curl in the subtropical region with a time lag of 0–2 years. A subsequent study using the 137°E data during 1967–1995 (Suga et al. 2000) showed that the area and S of NPTW ($S > 34.9$) increased remarkably in association with the 1976/77 regime shift (Nitta and Yamada 1989; Trenberth 1990; Fig. 8b). This change was explained only partly by the thermohaline forcing estimated from available evaporation and wind stress data, but was well explained by the Ekman pumping calculated from wind stress data.

A decade later, accumulation of Argo profiling float data and satellite altimeter sea surface height data as well as development of various surface flux data enabled us to fully examine variations in the NPTW formation and circulation with the underlying mechanisms. Katsura et al. (2013) analyzed Argo float data spanning 2003–2011 to demonstrate that the most saline portion of NPTW around 15°N in the 137°E section was formed in the western part of the sea surface S maximum near 25°N, 180°. In this part of the formation region, excess evaporation over precipitation seemed to be balanced by eddy diffusion, whose strength varied in association with the PDO (Qiu and Chen 2013; Sect. 4.2). As a result, the maximum S of NPTW in the 137°E during 1992–2012 lagged the PDO index by 3 years, which was considered to be the sum of 1 year for the eddy activity adjustment to the PDO forcing and 2 years for the NPTW advection. More recently, Nakano et al. (2015) analyzed the 137°E measurements spanning 1967–2011 to reveal that the decadal variability of NPTW area ($S > 34.9$) differed between its southern (and the most saline) part at 10°N–18°N and its northern part at 18°N–25°N, the latter of which dominated variability of the total area (Fig. 8b). The decadal variability of northern NPTW area was positively correlated with both evaporation over precipitation and Ekman pumping in the formation region west of 180°, and also with the PDO-related eddy kinetic energy in the STCC region (Qiu and Chen 2013). It might be also related to the decadal KE variability, as the area (Nakano et al. 2015; Fig. 8b) and S (Nan et al. 2015) of northern NPTW exhibited a similar decadal variability to the S of STMW mentioned above, at least after ~ 1990 (Oka et al. 2017).

Low-frequency variability of NPIW and its cause have also been investigated, commonly assuming that the distribution of NPIW in the 137°E section depends primarily on its westward advection in the subtropical gyre. Qiu and Joyce (1992) analyzed the 137°E data over 1967–1988 to demonstrate that the cross-sectional area of NPIW ($S < 34.25$) decreased during large-meander periods of the Kuroshio (Fig. 8c), as a result of weakening of the Kuroshio recirculation, as is the case with STMW. Shuto (1996), without considering the Kuroshio path state, indicated that decadal variability of NPIW area ($S < 34.2$) corresponded to that of the absolute maximum of negative wind stress curl with a time lag of 3–6 years. Nakano et al. (2005) used the 137°E data up to 2000 to exhibit that the NPIW area ($S < 34.2$), which had dominant time scales of 10 and 3–4 years, was correlated with the North Pacific index (Trenberth and Hurrell 1994) representing the strength of the Aleutian Low with a lag of about 11 years on decadal time scales, and with wind stress curl in the central North Pacific with a time lag of 4 years on interannual time scales. More recently, Sugimoto and Hanawa (2011) analyzed the 137°E section during 1972–2008 to demonstrate that the decadal variability of NPIW area ($S < 34.2$) was dominated by that of its northern part north of 25°N (Fig. 8c), which corresponded to the intensity of the Kuroshio recirculation that fluctuated as the first-mode baroclinic response to the Aleutian Low activity.

Generally speaking, it is becoming increasingly clear when reviewing recently published studies (Sugimoto and Hanawa 2011; Nakano et al. 2015; Oka et al. 2015, 2017) that decadal variability of the KE system commonly influences characteristics of STMW, NPTW, and NPIW, whose cross-sectional area in the 137°E section simultaneously increases (decreases) during stable (unstable) KE periods characterized by strengthened (weakened) recirculation gyre and low (high) eddy activity. In Fig. 8, such synchronized decadal variability seems to exist to some extent for the last 25 years since 1992, during which the KE path has been monitored by satellite altimeter measurements and the Kuroshio has mostly taken a non-large-meander path. This is an interesting relation that needs quantification in a future study because if true, the decadal variability of representative water masses in the 137°E section is controlled by oceanic processes rather than local air–sea processes, and is remotely controlled by the PDO-related atmospheric forcing in the central North Pacific.

The 137°E section has also contributed to clarifying long-term T and S changes. In the North Pacific subtropical gyre, a freshening trend has been widely observed in the main thermocline/halocline and the underlying NPIW and TSM (e.g., Lukas 2001; Wong et al. 2001; Ren and Riser 2010) as a part of global change (e.g., Wong et al. 1999; Hosoda

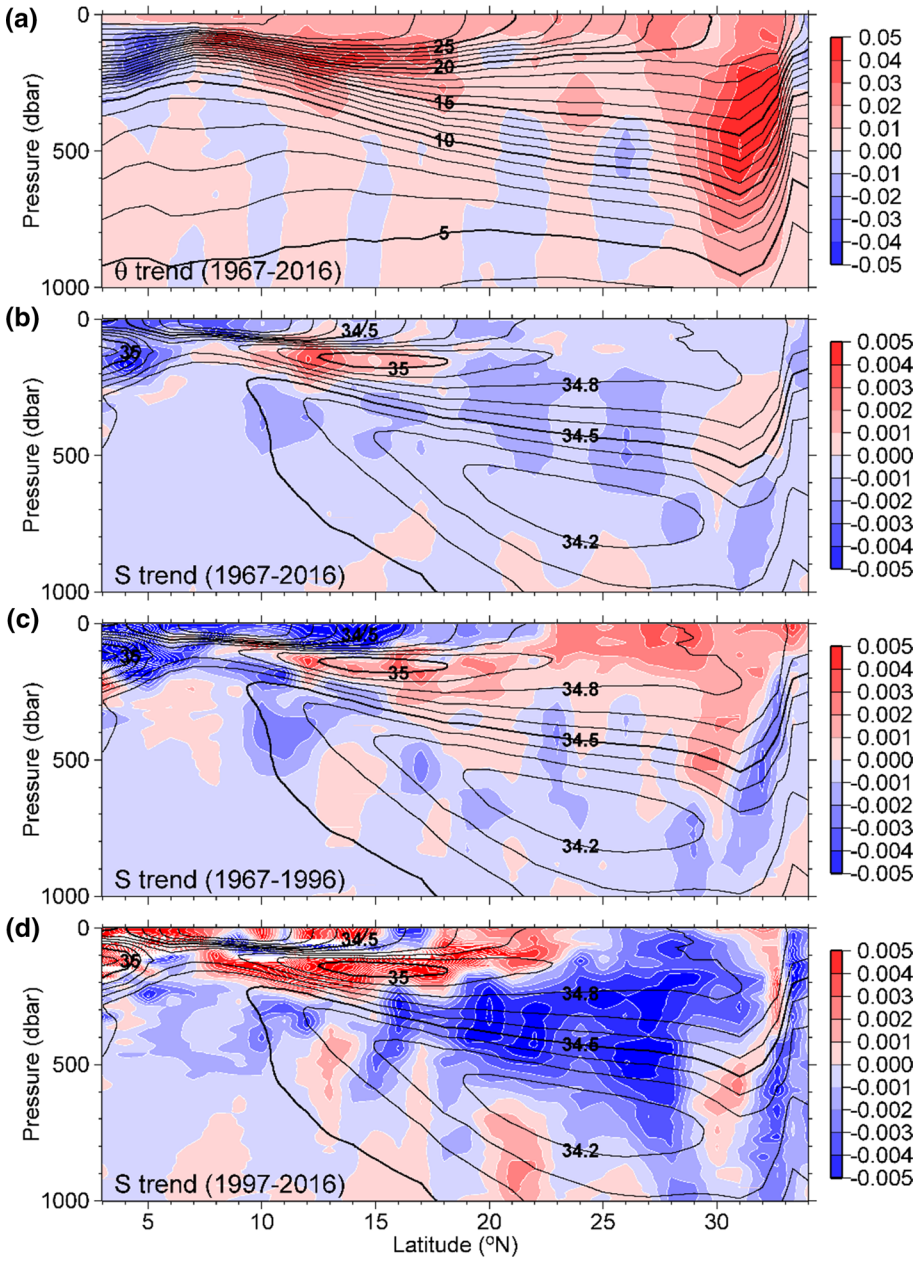

Fig. 9 Average (black contour; units °C in **a**) and linear trend (white contours with color; units °C year^{-1} in **a** and year^{-1} in **b**) of **a** θ and **b** S with respect to pressure in the 137°E section during 1967–2016. Linear trend of S during **c** 1967–1996 and **d** 1997–2016, otherwise following **b** (modified after Oka et al. 2017)

et al. 2009; Durack and Wijffels 2010). Nakano et al. (2007) analyzed the 137°E section during 1967–2005 to report an isobaric freshening trend reaching − 0.0015 year^{-1} from the lower thermocline/halocline to NPIW/TSM. On the other hand, Qiu and Chen (2012) and Nan et al. (2015) used more recent time series during 1993–2009 and 1992–2009, respectively, to present a freshening trend several times larger than Nakano et al.'s (2007) from the upper thermocline/halocline to the surface layer, which suggests interdecadal changes. The latest analysis of 50-year time series during 1967–2016 (Oka et al. 2017; Fig. 9) clarified that rapid freshening began in mid-1990s and persisted for the last 20 years in the upper halocline corresponding to STMW and a lighter variety of Central Mode Water (CMW; Nakamura 1996; Suga et al. 1997; Oka and Suga 2005). Additional analyses of the repeat hydrographic section along 144°E maintained by the Japan Coast Guard demonstrated that the freshening trend originated in the winter mixed layer in the KE region, although the mechanism of surface freshening in that region remains unclear. In association with this long-term freshening, the cross-sectional area of NPTW exhibits a trend toward decrease after the 1976/77 regime shift (Nakano et al. 2015; Fig. 8b), while that of NPIW shows a trend toward increase throughout the 50-year period (Fig. 8c).

In contrast with the freshening subtropics, T and S in the upper tropical ocean presented a large trend toward increase

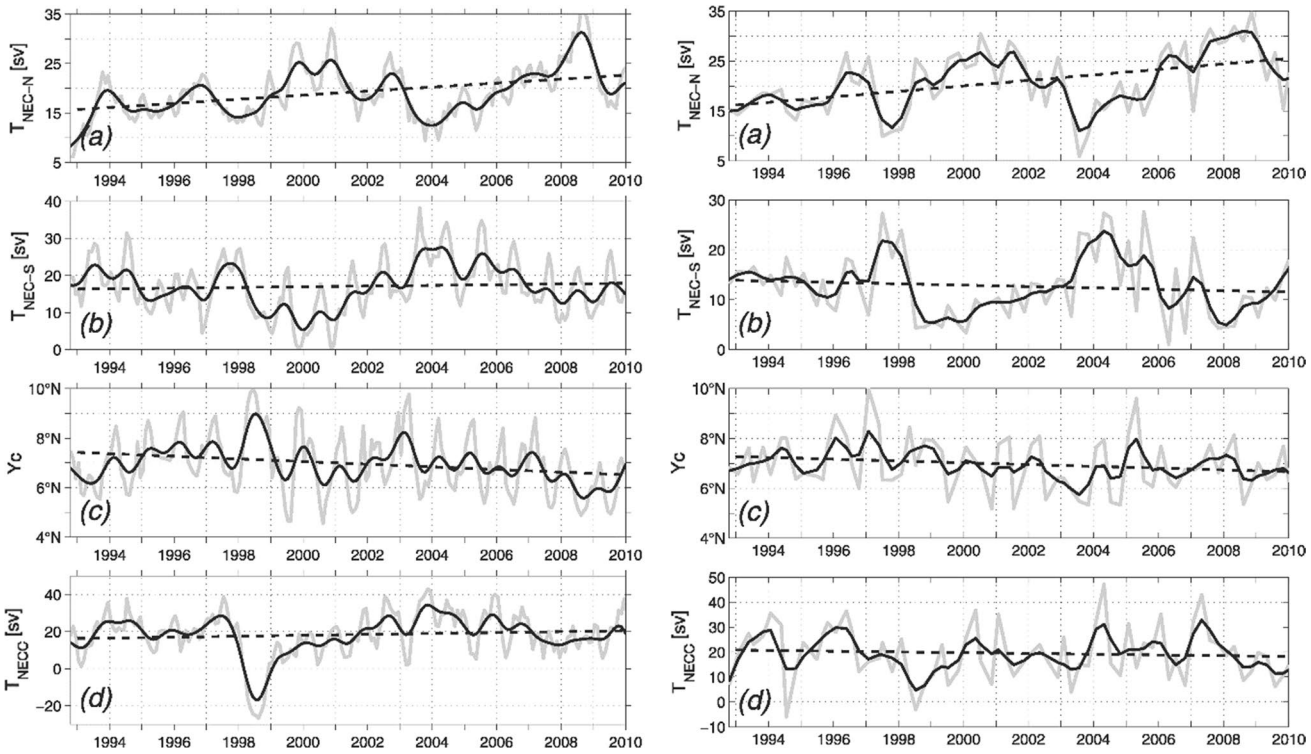

Fig. 10 Time series of **a** transport of the northern part of NEC circulating in the subtropical gyre, **b** transport of the southern part of NEC circulating in the tropical gyre, **c** the center latitude of the tropical gyre, and **d** the NECC transport based on the satellite altimeter data (left) and the quarterly 137°E section data (right). In the left (right) panels, gray line denotes the monthly (quarterly) values. In all panels, black line denotes the low-pass-filtered time series, and dashed line denotes the linear trend. Note that the increasing trend (4.1 Sv during 1993–2009) of the NECC transport detected by satellite altimeter data was not observed in the 137°E section data, presumably because of the local decreasing trend north of New Guinea (after Qiu and Chen 2012)

centered at 12°N, 150 dbar (Fig. 9a, b). This is primarily related to southward shift of NEC, whose thermosteric effect resulted in a local sea-level rise exceeding 10 mm year^{-1} that is more than three times faster than the global average (Qiu and Chen 2012; Sect. 4.2).

4.2 Large to mesoscale currents

Qiu and Joyce (1992) analyzed the 137°E section in winters of 1967–1988 and summers of 1972–1988 to examine variations of various currents and water masses. They argued that for El Niño years relative to non-El Niño years, surface dynamic height in the tropical region was lower, as previously reported for summer 1972 and winter 1973 (Masuzawa and Nagasaka 1975), geostrophic volume transport of both the NEC and the NECC was larger (71 and 69 Sv versus 57 and 42 Sv; 1 Sv $\equiv 10^6$ m^3 s^{-1}), and the boundary between the NEC and the NECC and the southern boundary of the NECC both shifted southward by 1°. They also demonstrated that the volume transport of the two currents agreed well in both amplitude and phase with the Sverdrup transport estimated from wind stress data.

Two decades later, bifurcation of the NEC at the eastern coast of the Philippines was examined by using satellite altimeter sea surface height data during 1993–2009 (Qiu and Chen 2010b). Interannual variation of the bifurcation latitude, which was much larger than its seasonal variation, corresponded well with the Niño-3.4 index, being higher in El Niño years with larger volume transport of both the NEC and the NECC. The satellite altimeter data and the

quarterly 137°E section data during 1993–2009 analyzed in a subsequent study (Qiu and Chen 2012) consistently demonstrated that over the 17 years the NEC bifurcation location and the boundary between the NEC and the NECC shifted southward by 2° and 1°, and the volume transport of the NEC and the NECC increased by 8 and 4 Sv, respectively (Fig. 10). Using a 1.5-layer reduced gravity model, Qiu and Chen (2012) concluded that the southward migration and the strengthening of the NEC/NECC accompanied by the rapid sea-level rise near the NEC bifurcation latitude (Sect. 4.1) were caused by the surface wind stress of the recently strengthened atmospheric Walker circulation. In support of this finding, Hu and Hu (2014) used ADCP data in the upper 200 m between 8°N and 18°N of the 137°E section during 1993–2008 to demonstrate that the volume transport of the NEC corresponded to the Niño-3.4 index with a time lag of 6 months and increased by 5 Sv over the 16 years. For longer time scales, Zhai et al. (2013) analyzed the 137°E section during 1972–2008 to indicate that the NEC transport exhibited decadal variability with a time scale of ~ 10 years in association with vertical movements of the sea surface and the permanent pycnocline in the southern part of the NEC, which was explained by decadal variability in the wind stress forcing. Such interannual to decadal variations and long-term changes of the NEC and the associated surface thermohaline structure likely impact the spawning of the Japanese eel (*Anguilla japonica*) near seamounts around 14°N, 143°E in the West Mariana Ridge (Fig. 1) and the subsequent larval transport to the growth habitats in East Asia (Tsukamoto 1992; Kimura et al. 1994, 2001; Kimura and Tsukamoto 2006; Tsukamoto 2006; Kim et al. 2007; Zenimoto et al. 2009; Hsu et al. 2017).

Since the STCC was discovered by Uda and Hasunuma (1969), its generation mechanism has been explored by many studies (Kobashi and Kubokawa 2012). Among them, Kubokawa and Inui (1999) and Kubokawa (1999) demonstrated using an idealized ocean general circulation model that low-PV waters with various densities subduct from the mixed layer depth front in the northern part of the subtropical gyre and pile up in the southern part of the gyre, and an eastward near-surface countercurrent is generated along the southern edge of this low-PV pool. In response to their numerical result, Aoki et al. (2002) analyzed four meridional repeat hydrographic sections including 137°E and the WHP one-time sections to examine the relation between two STCCs in the western North Pacific (Hasunuma and Yoshida 1978; Fig. 1) and mode waters (Oka and Qiu 2012). They concluded that the northern STCC was located at the southern edge of STMW, while the southern STCC was located at the southern edge of low-PV waters in a wide density range including CMW. Such correspondence between STCCs, including a third one in the eastern North Pacific, and mode waters was further demonstrated using climatology constructed from *T* profiles over the North Pacific (Kobashi et al. 2006).

The intensity of the STCC varies seasonally with a maximum in spring and a minimum in fall (White et al. 1978), largely because of the seasonal variation in the wind stress forcing (Takeuchi 1986). This alters the strength of baroclinic instability between the STCC and the NEC, resulting in the eddy kinetic energy in the STCC region (Fig. 5) being maximum in April–May and minimum in December–January (Qiu 1999; Kobashi and Kawamura 2002). To further reveal year-to-year variability of STCC's mesoscale eddy field, Qiu and Chen (2010a) analyzed satellite altimeter sea surface height data over 1993–2008 and demonstrated that eddy kinetic energy was higher in 1996–1998 and 2003–2008 and lower in the other years. They also examined the quarterly 137°E data during the same period to show that the vertical shear between the STCC and the NEC was larger and more favorable for baroclinic instability in eddy-rich years than eddy-weak years. Their subsequent study (Qiu and Chen 2013) revealed that decadal variability of eddy kinetic energy was highly correlated with the PDO index with a lag of 6 months and was due to the decadal variability of the vertical shear, which was controlled by that of surface heat flux forcing rather than wind stress forcing through convergence of Ekman heat flux.

Interannual variability in the volume transport of the Kuroshio and its relation to the path variations south of Japan (Fig. 1; horizontal bars at the bottom of each panel in Fig. 8) have also been the subject of broad interest. Qiu and Joyce (1992) analyzed the 137°E section over 1967–1988 to demonstrate that the net transport of the Kuroshio, which was defined as the eastward transport of the Kuroshio minus the westward transport of the Kuroshio Countercurrent, was larger during large-meander periods (39 Sv) than non-large-meander periods (29 Sv) on average. This supported observational results in the East China Sea (Kawabe 1980; Saiki 1982) and numerical results (Chao 1984; Yoon and Yasuda 1987; Akitomo et al. 1991), while recent sensitivity experiments using a data-assimilation model (Usui et al. 2013) indicated that smaller transport is favorable for maintenance of the large meander, as pointed out by earlier observational studies (e.g., Nan'niti 1960; Nitani 1975). For longer-term variations, Sugimoto et al. (2010) analyzed the 137°E section over 1972–2007 to demonstrate that the net Kuroshio transport varied on a time scale of ~ 10 years in association with vertical movements of the permanent pycnocline in the southern part of the Kuroshio, which fluctuated as the first-mode baroclinic response to the Aleutian Low activity. They also indicated that the transport of the Kuroshio recirculation also fluctuated decadally, affecting the cross-sectional area of NPIW in the 137°E section (Sugimoto and Hanawa 2011; Sect. 4.1).

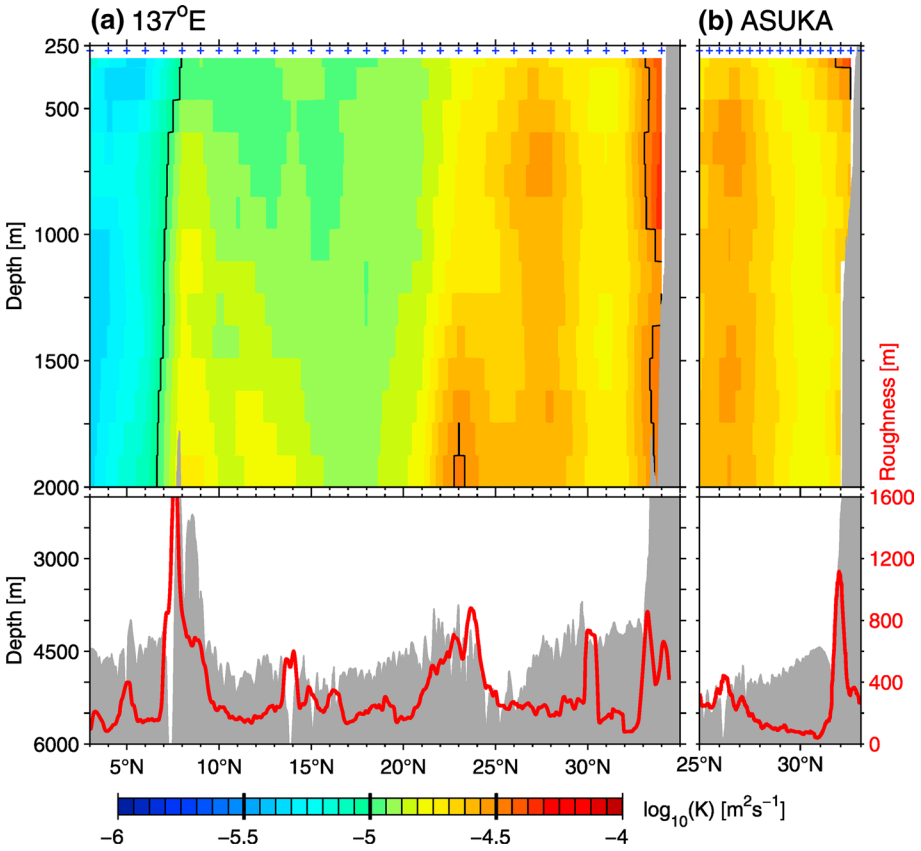

Fig. 11 **a** (Top) Distribution of time-mean diapycnal diffusivity (K) inferred from 57 CTD surveys at the 137°E section during 1997–2010. Gray shade denotes the bathymetry of Smith and Sandwell (1997). (Bottom) Red curve shows the roughness of bathymetry defined as the root-mean-square bathymetric height variance in a 32 km × 32 km square. **b** Distribution at the ASUKA section southeast of Shikoku, Japan, otherwise following **a** (after Qiu et al. 2012)

Several studies have analyzed the 137°E section to examine abyssal circulation in the Philippines Sea, where deep inflow through the channel at the junction of the Yap and West Mariana Ridges at 12°N, 139°E first enters the West Mariana Basin and then spreads northward to the Shikoku Basin and westward to the Philippines Basin (Mantyla and Reid 1983; Uehara and Taira 1990; Kawabe 1993; Fig. 1), as confirmed by the WHP full-depth observations including P9 (Kaneko et al. 1998, 2001). Sudo (1986) analyzed θ and dissolved O_2 data at 4000 m depth at 15, 20, 25, and 30°N during 1976–1983 and argued that property anomalies propagated from 15°N to 30°N in 1 year at a speed of 5–6 cm s^{-1}, while Fukasawa et al. (1995) subsequently reinterpreted the same θ time series as indicating that the anomalies propagated from 15°N to 30°N in 3 years at a speed of 2 cm s^{-1}. Further analyses of deep CTD casts continued at every 5° and the GO-SHIP P9 revisits in 2010 and 2016 (Fig. 3) are expected to clarify long-term variations of deep water properties and the abyssal circulation in the Philippines Sea.

4.3 Smaller-scale phenomena

Turbulent diapycnal mixing and its spatiotemporal variations, which control transport of heat, salt, and nutrients and maintain the ocean stratification, have drawn increasing attention in recent years (e.g., Wunsch and Ferrari 2004; Alford et al. 2016). Jing and Wu (2010) applied the Thorpe-scale (Thorpe 1977) and fine-scale parameterization (Kunze et al. 2006) methods to available CTD profiles at the 137°E section during 1998–2007 to examine the time-mean structure and seasonal variation of diapycnal mixing. Time-mean diapycnal diffusivity (K) exceeded 10^{-4} m^2 s^{-1} around 8°, 25°, and 34°N over the rough topography, and was 7.4×10^{-5} m^2 s^{-1} when averaged in the section at depths greater than 300 dbar, being much higher than the values of O (10^{-5} m^2 s^{-1}) obtained by microstructure measurements in the mid-latitude ocean interior (Gregg 1987). In addition, K in the Kuroshio region fluctuated seasonally with a maximum in winter and a minimum in spring and summer and decreased in amplitude with depth, presumably because of seasonally varying surface wind stress forcing. A subsequent study using CTD profiles at the JMA's three repeat sections including 137°E and the fine-scale parameterization method (Qiu et al. 2012) demonstrated that time-mean K at the 137°E section was high at 8°N–10°N, 22°N–24°N, 25°N–29°N, and 32°N–34°N (Fig. 11). The high K at the first two latitude bands over the rough topography was enhanced with depth, while that at 25°N–29°N over the relatively featureless topography, which was also observed at the other two sections, was vertically uniform and was attributable to parametric subharmonic instability. Lag-correlation analyses with external forcing indicated that the

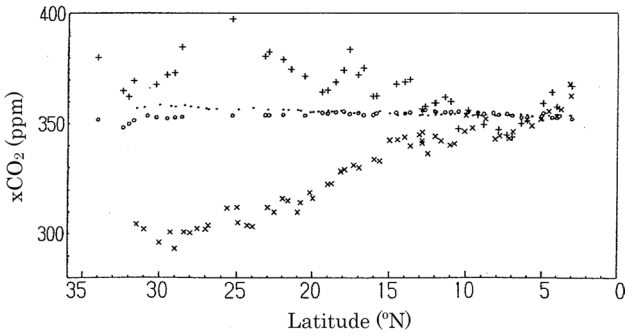

Fig. 12 CO_2 concentration (xCO_2) in surface seawater (cross, winter; plus, summer) and marine boundary air (dot, winter; circle, summer) along the 137°E section in winter and summer 1990, plotted against latitude (modified after Hirota et al. 1992). xCO_2 is related to pCO_2 as $pCO_2 = xCO_2$ (1 µatm − pH_2O), where pH_2O (µatm) is saturated water vapor pressure, which increases with temperature. As a result of the existence of pH_2O, pCO_2 values in µatm are 1–4% lower than xCO_2 values in ppm

time-varying K at 25°N–29°N corresponded to spring-neap modulated semidiurnal tidal current with a time lag of 6 days and to surface wind forcing with no time lag.

Submesoscale processes have also drawn increasing attention in recent years (e.g., Thomas et al. 2008; McWilliams 2016), and are expected to be further clarified by the onset of the Surface Water and Ocean Topography (SWOT) satellite mission planned for 2021, whose horizontal resolution (~ 15 km; Fu and Ubelmann 2014) is one order smaller than that of ongoing satellite observations (~ 150 km; Ducet et al. 2000). As satellite altimeter measurements detect signals of both balanced geostrophic flow that is dominant at meso and larger scales and unbalanced internal waves that are dominant at smaller scales, it is important for the SWOT mission to identify the length scale at which geostrophic flow loses its dominance and is overtaken by internal waves. To answer this question, Qiu et al. (2017) recently analyzed ADCP current velocity data in 33 surveys at the 137°E section to estimate the transition length scale in four latitude bands. Kinetic energy levels for internal waves were similar among the four bands, and those for geostrophic flow primarily determined the transition scale in each band. The estimated transition scale differed greatly among latitude bands, being 15 km in the eddy-abundant Kuroshio band (28°N–34°N), 50 and 80 km in the moderately unstable STCC (14°N–28°N) and NECC (3°N–9°N) bands, respectively, and 250 km in the stable NEC band (9°N–14°N).

5 Scientific achievements in biogeochemical oceanography

During and after the International Geophysical Year (1957–1958), it was found that CO_2 in surface seawater was in general not in equilibrium with that in marine boundary air (e.g., Torii et al. 1959; Takahashi 1961; Keeling 1968). To demonstrate the spatiotemporal variations of air–sea CO_2 exchange over the western North Pacific, the JMA measured the partial pressure of CO_2 in marine boundary air (pCO_2^{air})

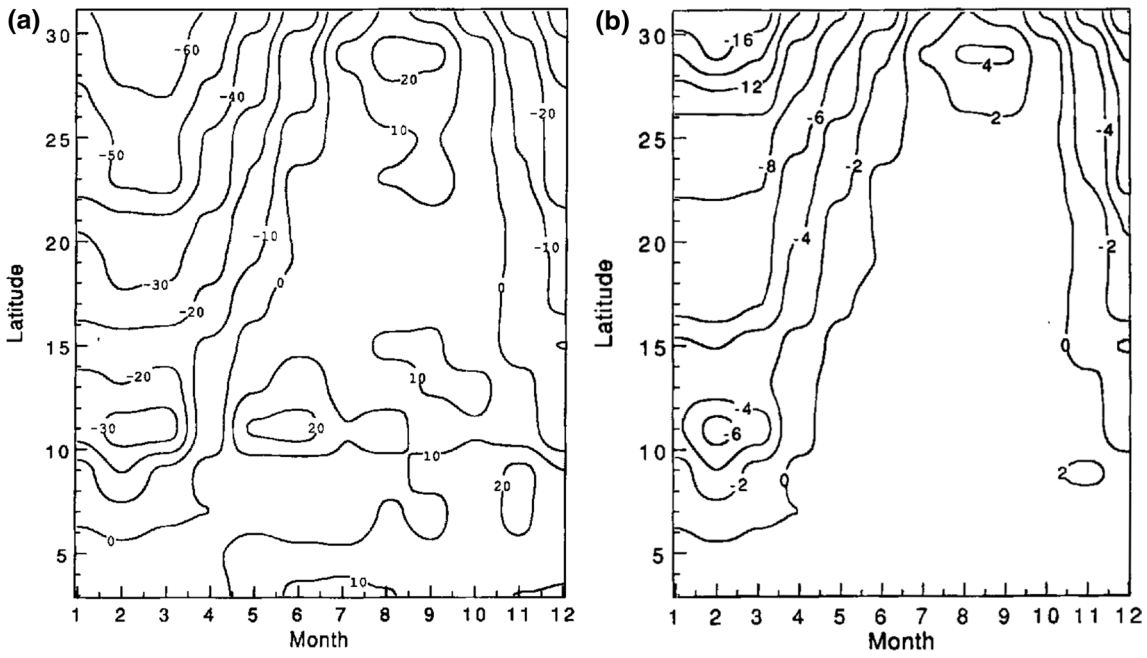

Fig. 13 Seasonal variation of **a** ΔpCO_2 (µatm) and **b** air–sea CO_2 flux (mmol m^{-2} day^{-1}) in the western North Pacific between 132°E and 142°E in 1990 (after Inoue et al. 1995)

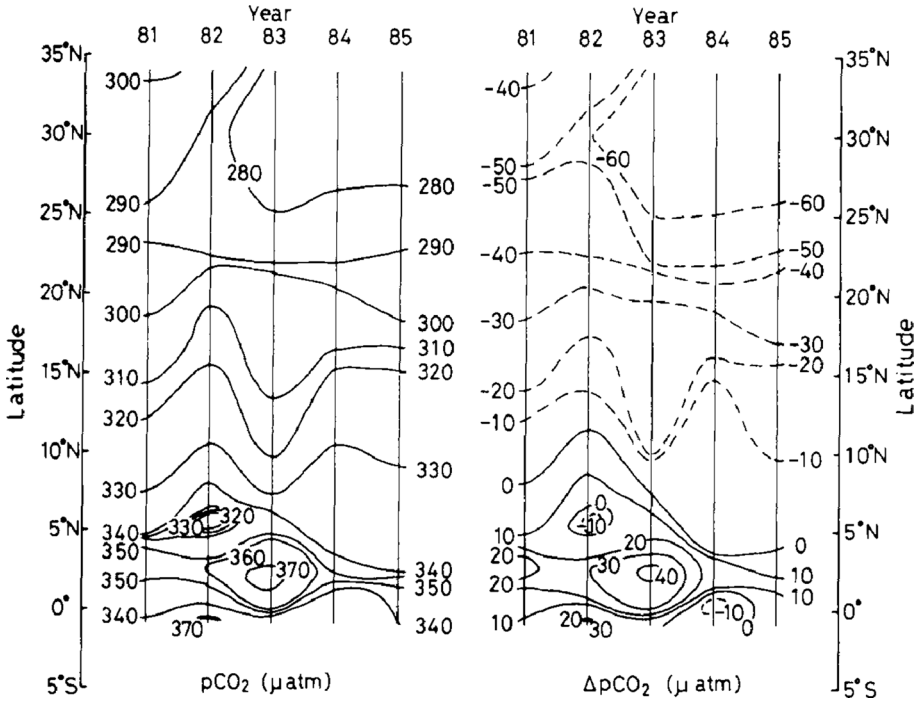

Fig. 14 Interannual variation of pCO_2^{sw} (left) and ΔpCO_2 (right) along the 137°E section in winter during 1981–1985 (after Fushimi 1987)

and that in an aliquot of air being equilibrated with surface seawater (pCO_2^{sw}) continuously along the 137°E section using a non-dispersive infrared gas analyzer and a shower-head-type equilibrator (Inoue 2000) for several winters from 1968 (Akiyama 1968, 1969; Masuzawa et al. 1970). After an interruption during the 1970s, the Meteorological Research Institute of the JMA, which had explored pCO_2 distributions in the Pacific, Indian, and Southern Oceans from the late 1960s to the early 1970s onboard R/V Hakuho-maru of the University of Tokyo (Miyake and Sugimura 1969; Miyake et al. 1974), resumed the pCO_2 measurements along the winter 137°E section for research purposes in 1981 (Fushimi 1987; Inoue et al. 1987). In the light of the importance of greenhouse gases in global warming (IPCC 1990), the JMA took over these measurements in 1990, by initiating biannual operational measurements of CO_2 in surface seawater and in the air as part of the Observation for Monitoring Background Marine Pollution (Hirota et al. 1991, 1992, 1993; Fushimi et al. 1993).

Measurements during the earlier years revealed that pCO_2^{sw} in the subtropical region exhibits large seasonal variations being low in winter and high in summer, and that this region serves as a strong sink of CO_2 on the annual average, which are now well known to the ocean carbon researchers. Along the winter 137°E section, pCO_2^{sw} is lowest at ~ 30°N in the subtropical region south of the Kuroshio and tends to be higher in the lower latitudes, while pCO_2^{air} shows smaller spatial variation, being nearly constant south of 15°N and increasing slightly northward north of 15°N (Fushimi 1987; Inoue et al. 1987; Fig. 12). Correspondingly, the difference between pCO_2^{sw} and pCO_2^{air} ($\Delta pCO_2 = pCO_2^{sw} - pCO_2^{air}$) is largely negative, reaching a minimum of – 60 μatm at ~ 30°N, and increases southward to around zero or even positive in the equatorial region. In summer, by contrast, pCO_2^{sw} is comparable to or higher by up to 50 μatm than pCO_2^{air}, which slightly decreases northward in the subtropical region (Hirota et al. 1991). The large seasonal variations of pCO_2^{sw} in the subtropics were attributed mainly to the thermodynamic effect of seasonal variation of sea surface temperature (SST) that is partly compensated for by the changes in carbon chemistry due to biological production in summer and by entrainment of CO_2-rich subsurface water in winter (Inoue et al. 1987, 1995; Inoue and Sugimura 1988a; Murata and Fushimi 1996; Murata et al. 1998; Fig. 13a). The net air–sea CO_2 flux (positive upward), which depends on ΔpCO_2 and the gas transfer velocity expressed as a function of wind speed, fluctuates seasonally in this region between − 16 mmol m^{-2} day^{-1} in winter, associated with large negative ΔpCO_2 and strong wind, and 4 mmol m^{-2} day^{-1} in summer (Inoue et al. 1995; Fig. 13b). For the annual average, the CO_2 flux is at a minimum of − 8 mmol m^{-2} day^{-1} south of the Kuroshio and increases southward, changing its sign at 5°N–10°N. In the equatorial region at 137°E located in the western equatorial Pacific warm pool, the annual-mean CO_2 flux range is 0.2–0.7 mmol m^{-2} day^{-1}, which indicates a weak CO_2 source. This source is much weaker than that in the upwelling region in the central and eastern equatorial Pacific known as the largest source in the world oceans (Tans et al. 1990).

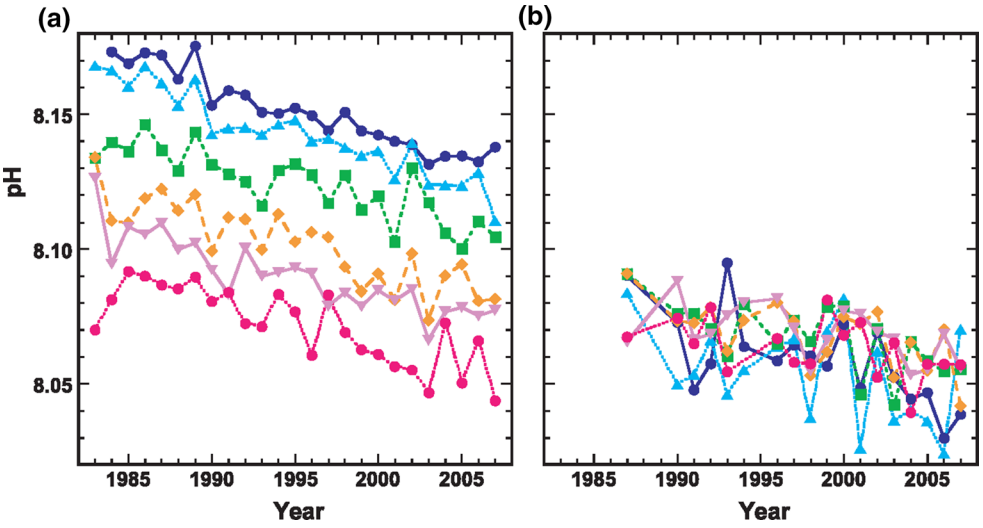

Fig. 15 Time series of surface pH at six latitudes at the 137°E section in **a** winter and **b** summer. Red circles, 3°N; violet triangles, 10°N; orange diamonds, 15°N; green squares, 20°N; light blue triangles, 25°N; and blue circles, 30°N (after Midorikawa et al. 2010)

In the equatorial region, pCO_2^{sw} and ΔpCO_2 fluctuate interannually in relation to ENSO. The pCO_2 measurements along the winter 137°E section from 1981 to 1985 revealed that in winter 1983 during the 1982/83 El Niño event, pCO_2^{sw}, and ΔpCO_2 between 1°S and 7°N considerably increased in association with SST decrease, presumably because of shallowing of the thermocline, while those between 7°N and 17°N decreased with SST (Fushimi 1987; Inoue et al. 1987; Fig. 14). This contrasted with the central and eastern equatorial Pacific during the same period where pCO_2^{sw} decreased to the values almost equivalent to those of pCO_2^{air} as a result of the cessation of upwelling (Feely et al. 1987). Subsequent measurements repeated in the western and central Pacific during 1987–1989 using several Japanese vessels demonstrated that pCO_2^{sw} in the central equatorial Pacific decreased in January and February 1987 during the 1986/88 El Niño event and increased in January and February 1989 during the 1988/89 La Niña event, while pCO_2^{sw} at the 137°E section in the western equatorial Pacific warm pool exhibited relatively small variations, compared to those during the strong 1982/83 El Niño event (Inoue and Sugimura 1988b, 1992). Furthermore, extensive pCO_2 measurements conducted over the entire equatorial Pacific during the 1990s as part of the Joint Global Ocean Flux Study showed that during the strong El Niño events, pCO_2^{sw} increased in the western equatorial Pacific but decreased to the near-equilibrium values in the central and eastern equatorial Pacific, resulting in the reduction of annual-mean CO_2 emission from the equatorial Pacific to 0.2–0.4 Pg C year^{-1} that was much smaller than 0.8–1.0 Pg C year^{-1} during non-El Niño years (Feely et al. 2002).

In addition to its seasonal and interannual variations, a long-term trend toward pCO_2^{sw} increase in response to the pCO_2^{air} increase associated with anthropogenic CO_2 emissions has been observed at 137°E. On the basis of the decade-long record from the winter 137°E section[3] from 1984 to 1993, Inoue et al. (1995) demonstrated that pCO_2^{sw} was increasing at a rate of + 1.8 ± 0.6 µatm year^{-1} at 15°N–30°N, which was equal to the rate of pCO_2^{air} increase, and + 0.5 ± 0.7 µatm year^{-1} at 3°N–14°N. Apart from a few studies indicating a long-term pCO_2^{sw} increase using two observations a decade apart (e.g., Inoue and Sugimura 1988a), this was the first study that corroborated the trend toward pCO_2^{sw} increase based on time-series data from shipboard observations. A decade later, Midorikawa et al. (2005) reconfirmed the persistent trend toward pCO_2^{sw} increase; its rate for the two decades of 1984–2003 averaged between 3°N and 34°N at the winter 137°E section was + 1.7 ± 0.2 µatm year^{-1} and was comparable to that of pCO_2^{air} (+ 1.60 ± 0.03 µatm year^{-1}), which suggests that the western North Pacific Ocean responds rapidly to the increase of CO_2 in the atmosphere.

The carbonate system in seawater is characterized by four measurable parameters: pCO_2, dissolved inorganic carbon (DIC), total alkalinity (TA), and pH. In principle, data of any two of these parameters and those of T and S can be used to derive the other carbonate system parameters. The JMA has measured DIC from discrete water samples at the 137°E section using a CO_2 extraction-coulometry method (Ishii et al. 1998) in summer 1994 (WHP P9), winter 1997, and summer 2000, and every cruise since 2003. On the basis of the data from five meridional transects in the western North Pacific during 1994–1997 including the above two at 137°E, Ishii et al. (2001) demonstrated that surface TA normalized at $S = 35$ (nTA), which was calculated from pCO_2^{sw}, surface normalized DIC (nDIC), SST, and sea surface salinity (SSS),

[3] pCO_2^{sw} data in 1981 and 1982 have not been used in Inoue et al. (1995) and the subsequent studies because of a technical problem in the measurements (Inoue et al. 1995).

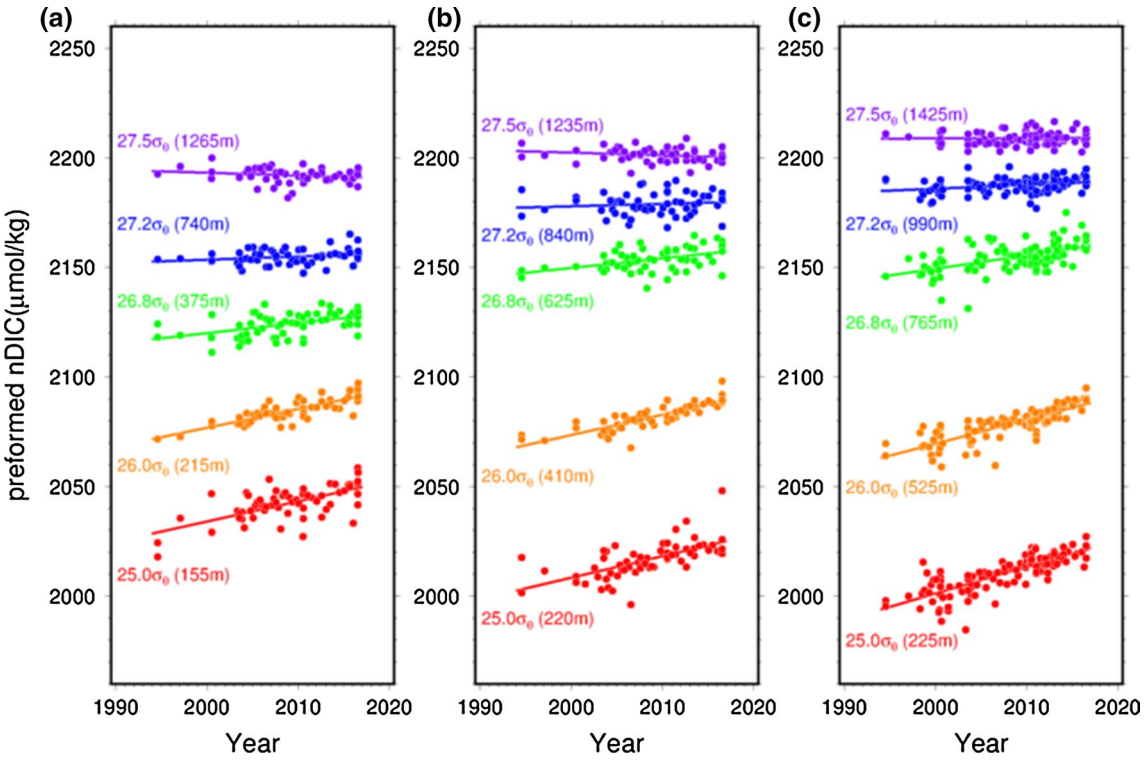

Fig. 16 Time series of preformed nDIC on the isopycnals of σ_θ = 25.0 (red), 26.0 (orange), 26.8 (green), 27.2 (blue), and 27.5 kg m^{-3} (purple) at **a** 10°N, **b** 20°N, and **c** 30°N of the 137°E section. Lines indicate the least-square fit. Values in parentheses denote the approximate depth of the isopycnals (after Japan Meteorological Agency 2017)

was almost invariable in space and time. They also indicated that the seasonal variations in pCO_2^{sw} were ascribed mainly to those of SST and nDIC; specifically, surface nDIC decreased (increased) from winter (summer) to summer (winter), compensating for ~ 30% of pCO_2^{sw} increase (decrease) due to SST increase (decrease). Furthermore, Ishii et al. (2001) estimated the monthly surface nDIC distribution in the western subtropical gyre from pCO_2^{sw} and SST of Inoue et al. (1995) (Fig. 13a) assuming constant nTA. They diagnosed that the nDIC decrease from winter to summer was due to biological production and was partly compensated for by the air-to-sea CO_2 flux, while its increase from summer to winter was explained by entrainment of subsurface water associated with mixed layer deepening, and that the effect of the horizontal DIC transport appears minor. Their analysis was substantially applied to the measurements along the winter 137°E section over 1983–2003 by Midorikawa et al. (2006). On interannual time scales, the effects of SST and nDIC variations on pCO_2^{sw} variations in the subtropical region have been compensating for each other through entrainment, thereby allowing the long-term trend toward pCO_2^{sw} increase to be observed distinctly. This was also the case for the warm pool of the equatorial region where SST tends to be higher and DIC tends to be lower when stratification was enhanced by the formation of barrier layers (Lukas and Lindstrom 1991), although the relationship between SST change and DIC change was not so robust there (Ishii et al. 2009).

The JMA also started high-precision measurements of pH in 2003 (Saito et al. 2008) and TA in 2010 using indicator dye-spectrophotometry methods. Data of surface pH during 2003–2008 calculated from pCO_2^{sw}, SST, and SSS assuming a constant nTA agreed well with those measured spectrophotometrically when using dissociation constants of carbonic acid given by Lueker et al. (2000). This allowed the pH time series to be extended back to 1983 on the basis of pCO_2^{sw} measurements (Midorikawa et al. 2010). The calculated surface pH at 3°N–33°N of the 137°E section in winter (summer) during 1983–2007 (1987–2007) exhibited a long-term trend toward decrease at a rate of − 0.0018 ± 0.0002 year^{-1} (− 0.0013 ± 0.0005 year^{-1}) on average at ambient SST (Fig. 15) and that of − 0.0015 ± 0.0003 year^{-1} (− 0.0014 ± 0.0004 year^{-1}) when normalized to 25 °C. These trends were comparable to those observed at the time-series stations in the central subtropical North Pacific near Hawaii and those in the subtropics of the North Atlantic (Bates 2007; González-Dávila et al. 2007; Dore et al. 2009). A similar pH trend of − 0.0020 ± 0.0007 year^{-1}, together with a trend of − 0.012 ± 0.005 year^{-1} for the aragonite saturation state, was determined for 1994–2008 at the

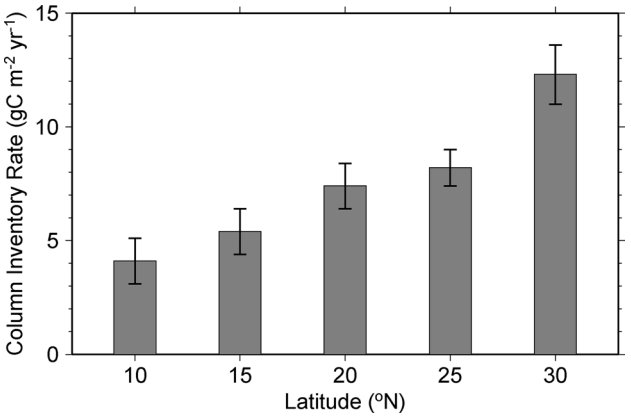

Fig. 17 Increasing rates of water column inventories of CO_2 between the sea surface and $\sigma_\theta = 27.5$ kg m^{-3} at 10°N–30°N of the 137°E section. Vertical bars indicate the 95% confidence interval (Replotted from Japan Meteorological Agency (2017)

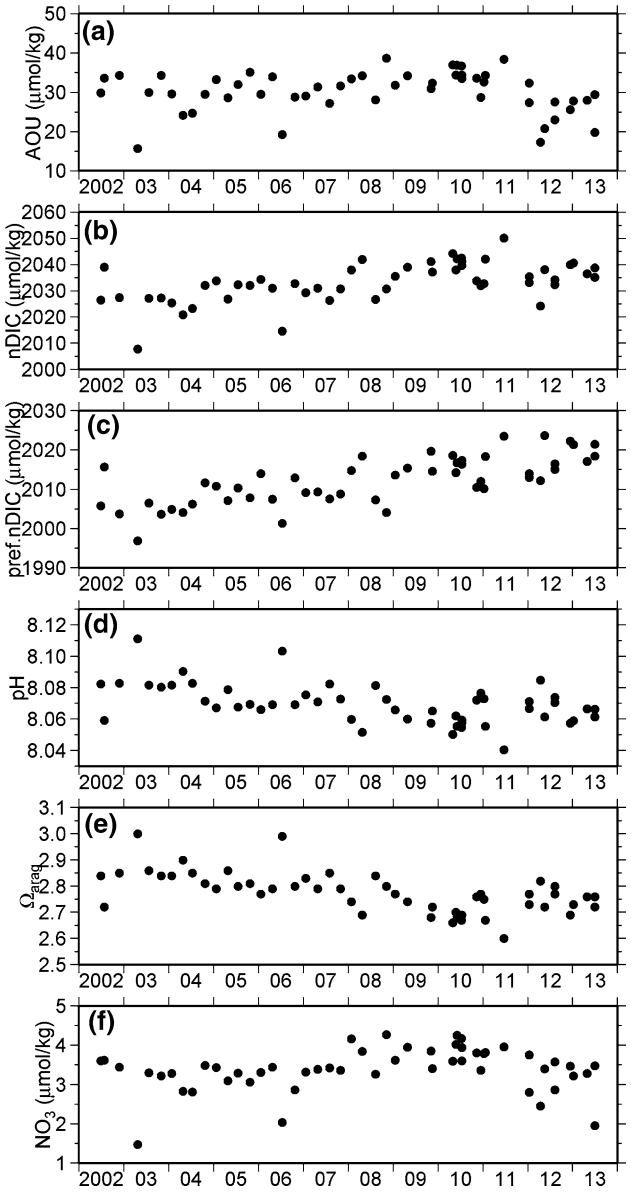

Fig. 18 Time series of **a** AOU, **b** salinity-normalized dissolved inorganic carbon (nDIC), **c** preformed nDIC, **d** pH, **e** aragonite saturation state index (Ω_{arag}), and **f** nitrate (NO_3) concentration on the isopycnal of $\sigma_\theta = 25.0$ kg m^{-3}, based on observations at 25°N of the 137°E section (after Oka et al. 2015)

northernmost stations (33°40′N–34°N) of the 137°E section located off the southern coast of Japan and inshore of the Kuroshio (Ishii et al. 2011).

Midorikawa et al. (2011) subsequently suggested the acceleration of ocean acidification after the 1980s by demonstrating that, when the trend toward surface pH decrease determined at the winter 137°E section over 1983–2008 was extrapolated back to 1969–1970, the extrapolated pH value at each latitude was higher than that estimated from the pCO_2^{sw} measurements made in the winter of these years along 138°E and 158°E (Miyake et al. 1974; Inoue et al. 1999). On the other hand, Midorikawa et al. (2012) pointed out that in spite of the acceleration of pCO_2^{air} increase over the long term, the mean rate of pCO_2^{sw} increase at the winter 137°E section was lower for 1999–2009 than for the earlier period of 1984–1997 at most latitudes between 3°N and 33°N. This was particularly the case at 10°N–20°N where the southward migration of NEC (Qiu and Chen 2012; Sect. 4.2) possibly led to thickening of the warm and CO_2-poor surface water and the reduction of entrainment of CO_2-rich subsurface water. Thus, the rate of pCO_2^{sw} increase was likely to be decadally variable, and its mechanism needs to be pursued in a future study.

As a result of subduction from the winter mixed layer with increasing pCO_2^{sw}, DIC in the ocean interior has been increasing. In the latest issue of the annual Marine Diagnosis Report (Japan Meteorological Agency 2017), it is shown that nDIC at the 137°E section exhibits a long-term trend toward increase on isopycnals down to $\sigma_\theta = 27.2$ kg m^{-3} for the last two decades (Fig. 16). In the water column between the sea surface and $\sigma_\theta = 27.5$ kg m^{-3} at a depth of ~ 1300 m, anthropogenic CO_2 has been accumulated at a mean rate of 4.1–12.3 gC m^{-2} year^{-1} over 1994–2016 (Fig. 17). The accumulation rate was highest at 30°N, where STMW that transports CO_2 from the surface layer to the interior is thickest. In addition to this long-term change, PDO-related decadal variability of STMW formation and subduction (Sect. 4.1) influences biogeochemical structure in the upper part of the permanent thermocline in the western subtropical gyre. By analyzing biogeochemical data at 25°N in the 137°E section, Oka et al. (2015) detected consistent changes during the stable KE period after 2010 that pH and aragonite saturation state (AOU, nitrate, and

nDIC) in the STMW layer increased (decreased), particularly against long-term trends for pH, aragonite saturation state, and nDIC, in association with the increasing advection of STMW from the east (Fig. 18). This result indicates a new mechanism by which climate variability impacts biogeochemical properties in the ocean's interior, and potentially also impacts the surface ocean acidification trend along with biological productivity.

Along with the ocean acidification, decrease of O_2 concentration in seawater, i.e., deoxygenation, associated with the ocean warming is another potential threat to marine ecosystems. Takatani et al. (2012) analyzed the 137°E section over 1967–2010 to investigate the trend of dissolved O_2 on isopycnals. They found marked decreases of O_2 at 20°N–25°N in the subtropical gyre after the mid-1980s, with a rate of -0.28 ± 0.08 μmol kg^{-1} year^{-1} on $\sigma_\theta = 25.5$ kg m^{-3} (corresponding to the denser limit of STMW), -0.36 ± 0.08 μmol kg^{-1} year^{-1} on 26.8 kg m^{-3} (NPIW), and -0.23 ± 0.04 μmol kg^{-1} year^{-1} on 27.3 kg m^{-3} (O_2 minimum layer). They demonstrated that the O_2 decrease in the upper pycnocline (< 26.0 kg m^{-3}) was due mainly to the isopycnal deepening and the decline of O_2 solubility associated with upper ocean warming, while that in the layers below (> 26.0 kg m^{-3}) was attributable primarily to AOU changes; specifically, the O_2 decrease in the NPIW originated from the NPIW formation region, and that in the O_2 minimum layer was explained by intensification of westward transport of low O_2 water from the eastern North Pacific.

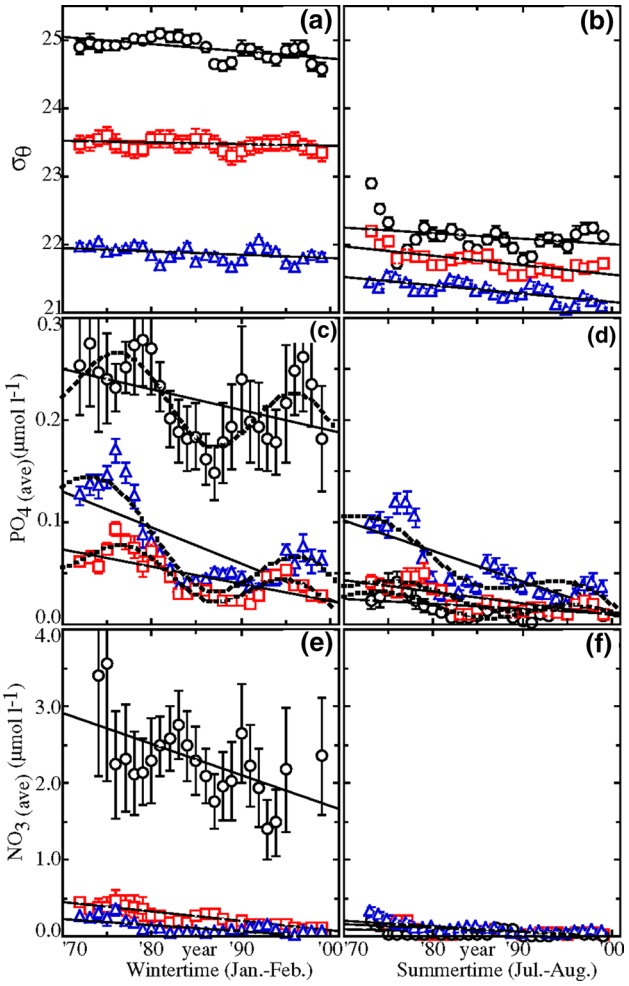

Fig. 19 Time series of the mixed layer σ_θ (**a**, **b**) and phosphate (PO_4; **c**, **d**) and nitrate (NO_3; **e**, **f**) averaged in the mixed layer at 30°N–34°N (black circles), 15°N–30°N (blue triangles), and 3°N–15°N (red squares) of the 137°E section in winter (**a**, **c**, **e**) and summer (**b**, **d**, **f**). Vertical bars denote standard errors for 3-year running mean. Solid lines and dashed curves represent the linear regression line and the nonlinear fitting curve estimated by the Fourier sine expansion, respectively (after Watanabe et al. 2005)

6 Scientific achievements in other research areas

6.1 Biological oceanography

Phytoplankton and zooplankton sampling along the 137°E section was conducted from 1967 through 2006. Phytoplankton in water samples from Nansen or Niskin bottles, mainly diatoms, were concentrated by decanting and centrifugalizing, and were identified and counted using a light microscope (Kawarada et al. 1968). Macrozooplankton was collected by vertically towing a 0.33-mm-mesh NORPAC net with a 45-cm-diameter aperture and a 180-cm length from 150 m depth to the sea surface, and chaetognaths and some copepods were identified and counted using a stereomicroscope (Kawarada et al. 1968; Kitou 1974; Kawashima and Nagai 1990; Nagai et al. 2015). In the CSK cruise in January–March 1967 including the first 137°E section (Masuzawa 1967), a new species of calanoid Copepoda, *Calanoides philippinensis* (Kitou and Tanaka 1969), was described.

Along the 137°E section, both diatoms and chaetognaths were abundant in the Kuroshio and the equatorial regions, while they were scarce in the NEC (Kawarada et al. 1968). The latest analysis for winter observations during 1967–1995 (Nagai et al. 2015) recorded 26 chaetognath species, of which 22 were epipelagic and 4 were mesopelagic, and classified 17 common epipelagic species into six groups according to their distributions: *Zonosagitta nagae* in the Japanese coast type, *Mesosagitta minima* in the Japanese coast-Kuroshio type, *Krohnitta subtilis*, *Pseudosagitta lyra*, *Sagitta bipunctata*, and *Serratosagitta pseudoserratodentata* in the Kuroshio-subtropical type, *Aidanosagitta neglecta*, *Ferosagitta ferox*, *Fe. robusta*, and

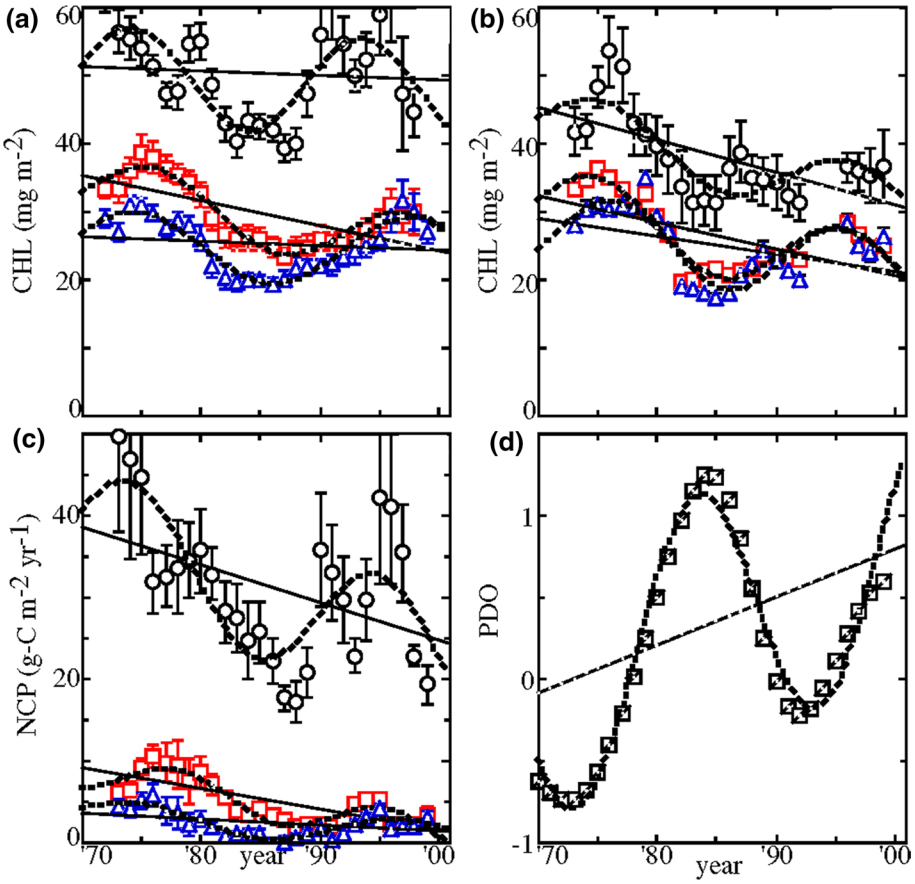

Fig. 20 Time series of the water column Chl-*a* (CHL) in **a** winter and **b** summer and **c** net community production (NCP) at the 137°E section, otherwise following Fig. 19. **d** PDO index in winter (after Watanabe et al. 2005)

Flaccisagitta enflata in the NEC-NECC type, *A. regularis*, *K. pacifica*, *Z. bedoti*, and *Z. pulchra* in the NECC type, and *Fl. hexaptera*, *Pterosagitta draco*, and *Se. pacifica* in the bimodal type characterized by a bimodal distribution with the minimum in the NEC.

As with physical and biogeochemical parameters, biological properties have exhibited long-term variations and trends. Sugimoto and Tadokoro (1998) analyzed the 137°E section during 1970–1992 to demonstrate that the chlorophyll-*a* (Chl-*a*) concentration in the upper 200 m decreased drastically around 1980 in both winter and summer in all regions at 30°N–32°N, 21°N–23°N, and 14°N–16°N corresponding to the Kuroshio and its counter current, the STCC, and the NEC, respectively, and that the nighttime mesozooplankton biomass in the upper 150 m also decreased simultaneously in the first two regions. On the basis of the longer 137°E time series during 1971–2000, Watanabe et al. (2005) demonstrated that the mixed layer σ_θ as well as phosphate and nitrate averaged vertically in the mixed layer exhibited a trend toward decrease in both winter and summer and in all areas at 30°N–34°N, 15°N–30°N, and 3°N–15°N, suggesting a decrease in the supply of nutrients from the subsurface (Fig. 19). Consistently, the water column Chl-*a* and net community production also had a trend toward decrease in all areas (Fig. 20). Furthermore, phosphate, Chl-*a*, and net community production in all seasons and areas fluctuated bidecadally with a period of ~ 21 years, lagging behind the PDO index by 2 years (Figs. 19, 20). Vertical structure of biological properties is also changing; during 1972–1997, the proportion of Chl-*a* existing in the upper 75 m of water column (the depth of subsurface Chl-*a* maximum) in summer has decreased (increased) at a rate of − 0.4% year^{-1} (0.4 m year^{-1}) in the subtropical region of the 137°E section (Ishida et al. 2009).

6.2 Marine pollution

To evaluate over the global ocean the degree of petroleum contamination at the sea surface, the Marine Pollution (Petroleum) Monitoring Pilot Project (MaPPMoPP) was implemented by the Intergovernmental Oceanographic Commission and the World Meteorological Organization under the framework of the Integrated Global Ocean Station System in 1975–1980. In response to the request from the MaPPMoPP, the JMA started visual observations of floating pollutants such as floating plastics (Suzuoki and Shirakawa 1979) and oil slicks in 1976 and measurements of floating particulate petroleum residues (tar balls; Sano et al. 1979) and dissolved/dispersed petroleum hydrocarbons (Shigehara et al. 1979) in 1977 in the

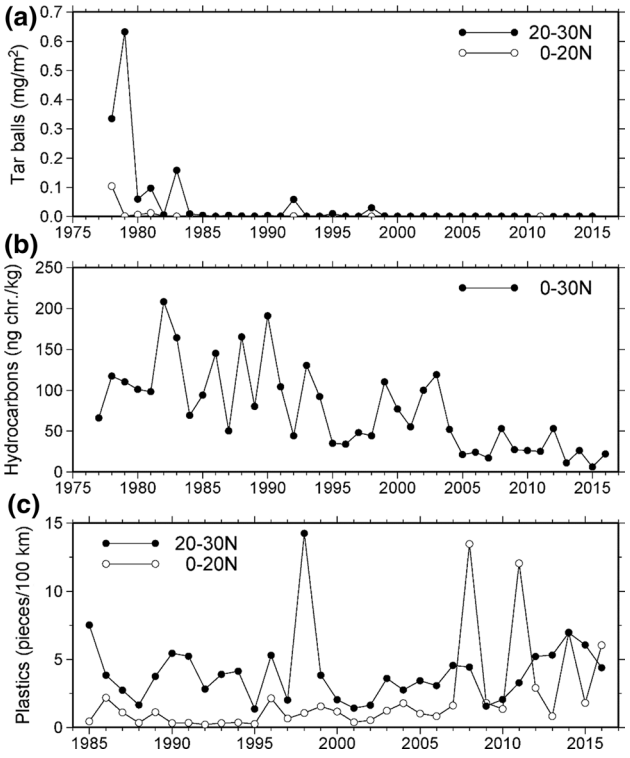

Fig. 21 Time series of annual-mean concentrations of **a** tar balls, **b** petroleum hydrocarbons as chrysene equivalent, and **c** floating plastics at the 137°E section. Replotted from Japan Meteorological Agency (2013) with additional data in 2013–2016 (Japan Meteorological Agency 2017)

western North Pacific including the 137°E section, as part of the Observation for Monitoring Background Marine Pollution (Ogawa and Takatani 1998; Takatani et al. 1999; Kamiya 2013). Observations during the earlier years demonstrated that tar balls, collected by Neuston net towed at the sea surface, and petroleum hydrocarbons, extracted from surface water using carbon tetrachloride and determined by fluorescence spectrophotometry, were abundant in the Kuroshio and its countercurrent, in the STCC, and north of New Guinea, while they were scarce in the NEC (Suzuoki and Matsuzaki 1983; Takatani et al. 1986). In addition, tar balls were sticky and shiny in the Kuroshio and became crumbly and dull to the south and the east, implying that they had been weathered while being transported from their likely source in the western margin of the western North Pacific where the traffic of oil tankers was busy. At 137°E, tar balls decreased drastically around 1980, and petroleum hydrocarbons have gradually decreased with interannual fluctuations, owing to the restriction of oil discharges from ships by Annex I of the International Convention for the Prevention of Pollution from Ships (MARPOL) 73/78 that entered into force in 1983 (Takatani et al. 1986, 1999; Japan Meteorological Agency 2013; Fig. 21). On the other hand, floating plastics do not exhibit a clear long-term trend, despite the ban of dumping plastics by Annex V of the MARPOL 73/78 Convention that came into force in 1988.

7 Summary

Hydrographic observations along the 137°E section have been repeated by the JMA using R/Vs Ryofu-maru and Keifu-maru biannually in winter since 1967 and in summer since 1972. These operational observations that have persisted for more than 50 years were initiated as part of the CSK (Masuzawa 1967), and have been maintained with an aim to detect long-term variations of oceanic conditions in the western North Pacific connected with climate change and to monitor background marine pollution (Shuto 1996) and more recently to evaluate changes in the carbon cycle and the mechanistic drivers (Nakano 2013). The data collected along 137°E have been analyzed not only by the JMA officers but also by scientists from various countries to quantify and understand seasonal to decadal variations and long-term changes of thermohaline structures (Sect. 4.1), large to mesoscale currents (Sect. 4.2), biogeochemical and biological properties (Sects. 5, 6.1), and marine pollutants (Sect. 6.2). Despite the concerns expressed by Dr. Masuzawa during the early years regarding its sampling frequency (Sect. 1), the 137°E section has been quite useful because it captures zonal integration of westward propagating Rossby signals during the course of which seasonal and shorter-term variations are cancelled out (Qiu and Chen 2010b).

When the 137°E section was initiated 50 years ago, shipboard observations were the main tool of ocean research. Since then, significant development has been made with other observing platforms and tools, including satellites, Argo, various datasets of the ocean interior structure and surface fluxes, and numerical models. The great expansion of observing platforms for oceanography over the last several decades has in fact enhanced and enriched the scientific opportunities afforded by the 137°E section itself and thereby the scientific value of the section, as new generations of researchers are able to return to the historical measurement record with new processes and time scale questions. This is reflected in the accelerated increase in scientific publications that incorporate measurements from 137°E (Fig. 2). The continued extension and maintenance of the time series has also provided unique opportunities for evaluating variability and transients on decadal and longer time scales over which the ocean plays a dominant role in the climate system. Furthermore, the introduction of CTD and ADCP measurements in the late 1980s opened the door to explorations of submesoscale and microscale phenomena (Sect. 4.3). Thus, beyond Dr. Masuzawa's expectation, the 137°E section has

contributed to understanding of variability on a wide range of spatiotemporal scales, and has developed into an irreplaceable platform for integrated, multidisciplinary ocean observations.

Recent findings on decadal variability of water masses and currents related to the PDO (Sects. 4.1, 4.2) and on smaller-scale phenomena (Sect. 4.3) strongly suggest that the 137°E section continues to be an essential component of a multi-platform observing system for physical oceanography. In other research areas, it is obviously a "gold mine". For example, the measurements along 137°E offer a unique opportunity for linking the more well-studied surface variations on ocean biogeochemistry with subsurface variability (Sect. 5). In addition, although the duration of biogeochemical and biological measurements is relatively short compared to physical oceanographic measurements, the mechanistic understanding of scales of variability inferred from the 137°E section will be important in the interpretation of repeat hydrographic measurements, where there are known issues with aliasing of high-frequency variability in the decadal sampling strategy. Thus, analyses of continued measurements along 137°E will be of value not only for clarifying long-term variations over the local region but also for clarifying scales of variability more generally. Deep measurements including the WHP/GO-SHIP P9 transects in 1994, 2010, and 2016 also need to be analyzed to examine decadal variability in the abyssal Philippines Sea. It is worth noting, finally, that the JMA has also maintained other repeat hydrographic sections, including the one along 165°E corresponding to the WHP/GO-SHIP P13 section (e.g., Kawabe and Taira 1998; Midorikawa et al. 2002; Oka and Suga 2005; Kouketsu et al. 2013; Qiu et al. 2012; Sasano et al. 2015). Integrated analyses of these sections will lead to comprehensive understanding of common, large-scale variability in the western North Pacific that Dr. Masuzawa targeted 50 years ago.

Acknowledgements The authors are respectful and grateful to the late Dr. Jotaro Masuzawa for his foresight and leadership to launch the 137°E section and to the present and past staff in the Marine Division of the Global Environment and Marine Department (and the former Division/Department) and the captains and crews of the R/Vs Ryofu-maru and Keifu-maru, the Japan Meteorological Agency for their long-term observation efforts. The authors also thank Michio Aoyama, Chihiro Kawamura, Fumiaki Kobashi, Hideki Nagai, Naoki Nagai, Hiroshi Ogawa, Keith Rodgers, Masaro Saiki, Kazuaki Tadokoro, Atsushi Tsuda, Hiroaki Saito (the editor), and two anonymous reviewers for helpful comments on the manuscript. This review is based on the presentations and discussion made in the symposium entitled "Fifty years of the 137°E repeat hydrographic section and the future sustained ocean observations in Japan", which was held on March 18, 2016 in Tokyo associated with the spring meeting of the Oceanographic Society of Japan.

References

Akamatsu H, Sawara T (1969) The preliminary report of the third cruise for CSK, January to March 1969. Oceanogr Mag 21:83–96

Akitomo K, Awaji T, Imasato N (1991) Kuroshio path variation south of Japan. 1. Barotropic inflow–outflow model. J Geophys Res 96:2549–2560

Akiyama T (1968) Partial pressure of carbon dioxide in the atmosphere and in sea water over the western North Pacific Ocean. Oceanogr Mag 20:133–146

Akiyama T (1969) Carbon dioxide in the atmosphere and in sea water over the western North Pacific Ocean. Oceanogr Mag 21:121–127

Akiyama T, Sagi T, Yura T (1968) On the distributions of pH in situ and total alkalinity in the western North Pacific Ocean. Oceanogr Mag 20:1–8

Alford MH, MacKinnon JA, Simmons HL, Nash JD (2016) Near-inertial internal gravity waves in the ocean. Annu Rev Mar Sci 8:95–123

Ando K, McPhaden M (1997) Variability of surface layer hydrography in the tropical Pacific Ocean. J Geophys Res 102:23063–23078

Andow T (1987) Year-to-year variation of oceanography sub-surface section along the meridian of 137°E. Oceanogr Mag 37:47–73

Aoki Y, Suga T, Hanawa K (2002) Subsurface subtropical fronts of the North Pacific as inherent boundaries in the ventilated thermocline. J Phys Oceanogr 32:2299–2311

Bakker DCE et al (2016) A multi-decade record of high-quality fCO_2 data in version 3 of the Surface Ocean CO_2 Atlas (SOCAT). Earth Syst Sci Data 8:383–413

Bates NR (2007) Interannual variability of the oceanic CO_2 sink in the subtropical gyre of the North Atlantic Ocean over the last 2 decades. J Geophys Res 112:C09013. https://doi.org/10.1029/2006JC003759

Bessho S (1995) Geostrophic balance of the western North Pacific tropical current. Geophys Mag Ser 2(1):1–4

Bingham FM, Lukas R (1995) The distribution of intermediate water in the western equatorial Pacific during January–February 1986. Deep Sea Res II 42:1545–1573

Bingham FM, Suga T, Hanawa K (2002) Origin of waters observed along 137°E. J Geophys Res 107:3073. https://doi.org/10.1029/2000JC000722

Cannon GA (1966) Tropical waters in the western Pacific Oceans, August–September 1957. Deep Sea Res Oceanogr Abstr 13:1139–1148

Cerovečki I, Giglio D (2016) North Pacific subtropical mode water volume decrease in 2006–09 estimated from Argo observations: influence of surface formation and basin-scale oceanic variability. J Clim 29:2177–2199

Chao SY (1984) Bimodality of the Kuroshio. J Phys Oceanogr 14:92–103

Chen R, Flierl GR, Wunsch C (2015) Quantifying and interpreting striations in a subtropical gyre: a spectral perspective. J Phys Oceanogr 45:487–506

Chen X, Qiu B, Du Y, Chen S, Qi Y (2016) Interannual and interdecadal variability of the North Equatorial Countercurrent in the Western Pacific. J Geophys Res 121:7743–7758

Cromwell T, Montgomery RB, Stroup EC (1954) Equatorial undercurrent in Pacific Ocean revealed by new methods. Science 119:648–649

Dore JE, Lukas R, Sadler DW, Church MJ, Karl DM (2009) Physical and biogeochemical modulation of ocean acidification in the central North Pacific. Proc Natl Acad Sci 106:12235–12240

Ducet N, Le Traon PY, Reverdin F (2000) Global high-resolution mapping of ocean circulation from TOPEX/Poseidon and ERS-1 and -2. J Geophys Res 105:19477–19498

Durack PJ, Wijffels SE (2010) Fifty-year trend in global ocean salinities and their relationship to broad-scale warming. J Clim 23:4342–4362. https://doi.org/10.1175/2010JCLI3377.1

Feely RA, Gammon RH, Taft BA, Pullen PE, Waterman LS, Conway TJ, Gendron JF, Wisegarver DP (1987) Distribution of chemical tracers in the eastern equatorial Pacific during and after the 1982–83 El Niño/southern oscillation event. J Geophys Res 92:6545–6558

Feely RA, Boutin J, Cosca CE, Dandonneau Y, Etcheto J, Inoue HY, Ishii M, Quéré CL, Mackey DJ, McPhaden M, Metzl N, Poisson A, Wanninkhof R (2002) Seasonal and interannual variability of CO_2 in the equatorial Pacific. Deep Sea Res II 49:2443–2469

Fine RA, Lukas R, Bingham FM, Warner MJ, Gammon RH (1994) The western equatorial Pacific: a water mass crossroads. J Geophys Res 99:25063–25080

Fu LL, Ubelmann C (2014) On the transition from profile altimeter to swath altimeter for observing global ocean surface topography. J Atmos Ocean Technol 31:560–568

Fujii M, Chai F, Shi L, Inoue HY, Ishii M (2009) Seasonal and interannual variability of oceanic carbon cycling in the western and central tropical–subtropical Pacific: a physical–biogeochemical modeling study. J Oceanogr 65:689–701

Fujii Y, Nakano T, Usui N, Matsumoto S, Tsujino H, Kamachi M (2013) Pathways of the north Pacific intermediate water identified through the tangent linear and adjoint models of an ocean general circulation model. J Geophys Res 118:2035–2051. https://doi.org/10.1002/jgrc.20094

Fukasawa M, Teramoto T, Taira K (1995) Hydrographic structure in association with deep boundary current in the north of the Shikoku Basin. J Oceanogr 51:187–205

Fushimi K (1987) Variation of carbon dioxide partial pressure in the western North Pacific surface water during the 1982/83 El Niño event. Tellus 39B:214–227

Fushimi K, Hirota M, Nemoto K, Murata AM (1993) Distribution of methane in the surface seawater and the air/sea flux over the western North Pacific. Oceanogr Mag 43:33–46

González-Dávila M, Santana-Casiano JM, González-Dávila EF (2007) Interannual variability of the upper ocean carbon cycle in the northeast Atlantic Ocean. Geophys Res Lett 34:L07608. https://doi.org/10.1029/2006GL028145

Gouriou Y, Toole J (1993) Mean circulation of the upper layers of the western equatorial Pacific Ocean. J Geophys Res 98:22495–22520

Gregg MC (1987) Diapycnal mixing in the thermocline: a review. J Geophys Res 92:5249–5286

Guan B (1986) Current structure and its variation in the equatorial area of the western North Pacific Ocean. Chin J Oceanol Limnol 4:239–255

Guo XY, Zhu XH, Long Y, Huang DJ (2013) Spatial variations in the Kuroshio nutrient transport from the East China Sea to south of Japan. Biogeosciences 10:6403–6417

Hanawa K (1987) Interannual variations of the winter-time outcrop area of subtropical mode water in the western North Pacific Ocean. Atmos Ocean 25:358–374

Hanawa K, Hoshino I (1988) Temperature structure and mixed layer in the Kuroshio region over the Izu Ridge. J Mar Res 46:683–700

Hanawa K, Talley LD (2001) Mode waters. In: Church J et al (eds) Ocean circulation and climate. Academic, London, pp 373–386

Hanawa K, Watanabe T, Iwasaka N, Suga T, Toba Y (1988) Surface thermal conditions in the western North Pacific during the ENSO events. J Meteorol Soc Jpn 66:445–456

Hasunuma K, Yoshida K (1978) Splitting the subtropical gyre in the western North Pacific. J Oceanogr Soc Japan 34:160–172

Hayashi K (2008) Should we treat any low-potential-vorticity water observed in the 137°E section as the North Pacific subtropical mode water? Weather Serv Bull 75(Sp):S97–S103 (in Japanese)

Hayashi S, Miyashita I, Fujita I (1968) Maritime meteorological summary of western North Pacific Ocean in winter. Oceanogr Mag 20:105–120

Hayashi S, Takano H, Yamashita A (1970) Maritime meteorological summary of the western North Pacific Ocean in the winters of 1967, 1968 and 1969. Oceanogr Mag 22:95–123

Hirota M, Nemoto K, Murata A, Fushimi K (1991) Observation of carbon dioxide concentrations in air and surface sea water in the western North Pacific Ocean. Oceanogr Mag 41:19–28

Hirota M, Nemoto K, Murata A, Fushimi K (1992) The observation of greenhouse gases and substances that deplete the ozone layer on board the Research Vessel Ryofu Maru of the Japan Meteorological Agency. Weather Serv Bull 59:145–159 (in Japanese)

Hirota M, Nemoto K, Murata AM, Fushimi K (1993) Observation of methane concentrations in air and surface sea water in the western North Pacific Ocean. Oceanogr Mag 43:21–31

Hood M, Fukasawa M, Gruber N, Johnson GC, Koertzinger A, Sabine C, Sloyan B, Stansfield K, Tanhua T (2009) Ship-based repeat hydrography: a strategy for a sustained global program. In: Hall J, Harrison DE, Stammer D (eds) OceanObs'09: sustained ocean observations and information for society, vol 2. ESA Publication, WPP-306, Venice, 21–25 September 2009. https://doi.org/10.5270/oceanobs09.cwp.44

Hosoda S, Suga T, Shikama N, Mizuno K (2009) Global surface layer salinity change detected by ARGO and its implication for hydrological cycle intensification. J Oceanogr 65:579–586

Hsu AC, Xue H, Chai F, Xiu P, Han YS (2017) Variability of the Pacific North Equatorial Current and its implications on Japanese eel (*Anguilla japonica*) larval migration. Fish Oceanogr 26:251–267

Hu D, Cui M (1991) The western boundary current of the Pacific and its role in the climate. Chin J Oceanol Limnol 9:1–14

Hu S, Hu D (2014) Variability of the Pacific North Equatorial Current from repeated shipboard acoustic Doppler current profiler measurements. J Oceanogr 70:559–571

Inoue HY (2000) CO_2 exchange between the atmosphere and the ocean: carbon cycle studies of the Meteorological Research Institute since. In: Handa N, Tanoue E, Hama T (eds) Dynamics and characterization of marine organic matter. Terra Scientific, Tokyo, pp 509–531

Inoue H, Sugimura Y (1988a) Distribution and variations of oceanic carbon dioxide in the western North Pacific, eastern Indian, and Southern Ocean south of Australia. Tellus 40B:308–320

Inoue H, Sugimura Y (1988b) Distribution of the pCO_2 in the surface seawater of the western and central equatorial Pacific during the 1986/87 El Niño/Southern Oscillation event. Geophys Res Lett 15:1499–1502

Inoue HY, Sugimura Y (1992) Variations and distributions of CO_2 in and over the equatorial Pacific during the period from the 1986/88 El Niño event to the 1988/89 La Niña event. Tellus 44B:1–22

Inoue HY, Sugimura Y, Fushimi K (1987) pCO_2 and $\delta^{13}C$ in the air and surface sea water in the western North Pacific. Tellus 39B:228–242

Inoue HY, Matsueda H, Ishii M, Fushimi K, Hirota M, Asanuma I, Takasugi Y (1995) Long-term trend of the partial pressure of

carbon dioxide (pCO_2) in surface waters of the western North Pacific, 1984–1993. Tellus 47B:391–413

Inoue HY, Ishii M, Matsueda H, Saito S, Midorikawa T, Nemoto K (1999) MRI measurements of partial pressure of CO_2 in surface waters of the Pacific during 1968 to 1970: re-evaluation and comparison of data with those of the 1980s and 1990s. Tellus 51B:830–848

IPCC (1990) Climate change: the intergovernmental panel on climate change scientific assessment. Cambridge University Press, Cambridge

IPCC (2013) Climate change 2013: the physical science basis. In: Working Group I contribution to the fifth assessment report of the intergovernmental panel on climate change. Cambridge University Press, Cambridge

Ishida H, Watanabe WY, Ishizaka J, Nakano T, Nagai N, Watanabe Y, Shimamoto A, Maeda N, Magi M (2009) Possibly of recent changes in vertical distribution and size composition of chlorophyll-a in the western North Pacific region. J Oceanogr 65:179–186

Ishii M, Inoue HY, Matsueda H, Tanoue E (1998) Close coupling between seasonal biological production and dynamics of dissolved inorganic carbon in the Indian Ocean sector and the western Pacific Ocean sector of the Antarctic Ocean. Deep Sea Res I 45:1187–1209

Ishii M, Inoue HY, Matsueda H, Saito S, Fushimi K, Nemoto K, Yano T, Nagai H, Midorikawa T (2001) Seasonal variation in total inorganic carbon and its controlling processes in surface waters of the western North Pacific subtropical gyre. Mar Chem 75:17–32

Ishii M, Inoue HY, Midoriakwa T, Saito S, Tokieda T, Sasano D, Nakadate A, Nemoto K, Metzl N, Wong CS, Feely RA (2009) Spatial variability and decadal trend of the oceanic CO_2 in the western equatorial Pacific warm/fresh water. Deep Sea Res II 56:591–606

Ishii M, Kosugi N, Sasano D, Saito S, Midorikawa T, Inoue HY (2011) Ocean acidification off the south coast of Japan: a result from time series observations of CO_2 parameters from 1994 to 2008. J Geophys Res 116:C06022. https://doi.org/10.1029/2010JC006831

Japan Meteorological Agency (2013) Marine diagnosis report, 2nd edn. http://www.data.jma.go.jp/kaiyou/shindan/sougou/index.html. Accessed 30 Aug 2017 (in Japanese)

Japan Meteorological Agency (2017) Marine diagnosis report. http://www.data.jma.go.jp/kaiyou/shindan/index.html. Accessed 30 Oct 2017 (in Japanese)

Jing Z, Wu L (2010) Seasonal variation of turbulent diapycnal mixing in the northwestern Pacific stirred by wind stress. Geophys Res Lett 37:L23604. https://doi.org/10.1029/2010GL045418

Kamiya H (2013) On the international cooperation on oceanographic and marine meteorological observation by research vessels. Weather Serv Bull 80(Sp):S125–S138 (in Japanese)

Kaneko I (1998) World Ocean Circulatino Experiment (WOCE). Weather Serv Bull 65(Sp):S159–S161 (in Japanese)

Kaneko I (2002) Results of WHP observations carried out by the JMA. Weather Serv Bull 69(Sp):S147–S160 (in Japanese)

Kaneko I, Takatsuki Y, Kamiya H, Kawae S (1998) Water property and current distributions along the WHP-P9 section (137°–142°E) in the western North Pacific. J Geophys Res 103:12959–12984

Kaneko I, Takatsuki Y, Kamiya H (2001) Circulation of intermediate and deep waters in the Philippine Sea. J Oceanogr 57:397–420

Karl D, Lukas R (1996) The Hawaii Ocean Time-series (HOT) program: background, rationale and field implementation. Deep Sea Res II 43:129–156

Katsura S, Oka E, Qiu B, Schneider N (2013) Formation and subduction of North Pacific tropical water and their interannual variability. J Phys Oceanogr 43:2400–2415

Kawabe M (1980) Sea level variations along the south coast of Japan and the large meander in the Kuroshio. J Oceanogr Soc Jpn 36:97–104

Kawabe M (1993) Deep water properties and circulation in the western North Pacific. In: Teramoto T (ed) Deep ocean circulation: physical and chemical aspects, vol 59. Elsevier Oceanography Series. Elsevier, Amsterdam, pp 17–37

Kawabe M (1995) Variations of current path, velocity, and volume transport of the Kuroshio in relation with the large meander. J Phys Oceanogr 25:3103–3117

Kawabe M, Taira K (1998) Water masses and properties at 165°E in the western Pacific. J Geophys Res 103:12941–12958

Kawarada Y, Sano A (1969) Distribution of chlorophyll and phaeophytin in the western North Pacific. Oceanogr Mag 21:137–146

Kawarada Y, Kitou M, Furukawa K, Sano A (1968) Plankton in the western North Pacific in the winter of 1967 (CSK). Oceanogr Mag 20:9–29

Kawashima K, Nagai N (1990) Distribution of planktonic chaetognaths in the western North Pacific. Oceanogr Mag 40:53–64

Keeling CD (1968) Carbon dioxide in surface ocean waters: 4. Global distribution. J Geophys Res 73:4543–4553

Kim H, Kimura S, Shinoda A, Kitagawa T, Sasai Y, Sasaki H (2007) Effect of El Niño on migration and larval transport of the Japanese eel (*Anguilla japonica*). ICES J Mar Sci 64:1387–1395

Kimura Y (1982) Short-term temperature variation along 137°E in the subtropical region of the western North Pacific. Oceanogr Mag 32:1–10

Kimura S, Tsukamoto K (2006) The salinity front in the North Equatorial Current: a landmark for the spawning migration of the Japanese eel (*Anguilla japonica*) related to the stock recruitment. Deep Sea Res II 53:315–325

Kimura S, Tsukamoto K, Sugimoto T (1994) A model for the larval migration of the Japanese eel: roles of the trade winds and salinity front. Mar Biol 119:185–190

Kimura S, Inoue T, Sugimoto T (2001) Fluctuation in the distribution of low-salinity water in the North Equatorial Current and its effect on the larval transport of the Japanese eel. Fish Oceanogr 10:51–60

Kitou M (1974) Chaetognatha. In: Marumo R (ed) Marine plankton. University Tokyo Press, Tokyo, pp 65–85 (in Japanese)

Kitou M, Tanaka O (1969) Note on a species of *Calanoides* (Copepoda, Calanoida) from the western North Pacific. Oceanogr Mag 21:67–81

Kobashi F, Kawamura H (2002) Seasonal variation and instability nature of the North Pacific subtropical countercurrent and the Hawaiian Lee countercurrent. J Geophys Res 107:3185. https://doi.org/10.1029/2001JC001225

Kobashi F, Kubokawa A (2012) Review on North Pacific Subtropical Countercurrent and subtropical front: role of mode water in ocean circulation and climate. J Oceanogr 68:21–43

Kobashi F, Mitsudera H, Xie SP (2006) Three subtropical fronts in the North Pacific: observational evidence for mode water-induced subsurface frontogenesis. J Geophys Res 111:C09033. https://doi.org/10.1029/2006JC003479

Kouketsu S, Doi T, Murata A (2013) Decadal changes in dissolved inorganic carbon in the Pacific Ocean. Global Biogeochem Cycles 27:65–76

Kubokawa A (1999) Ventilated thermocline strongly affected by a deep mixed layer: a theory for subtropical countercurrent. J Phys Oceanogr 29:1314–1333

Kubokawa A, Inui T (1999) Subtropical countercurrent in an idealized ocean GCM. J Phys Oceanogr 29:1303–1313

Kunze E, Firing E, Hummon JM, Chereskin TK, Thurnherr AM (2006) Global abyssal mixing inferred from lowered ADCP shear and CTD strain profiles. J Phys Oceanogr 36(8):1553–1576

Kurihara K (1984) Analysis of the statistical relationship between the end of the Baiu in Tokyo and sea water temperatures in the western tropical Pacific Ocean. Geophys Mag 41:159–171
Kurihara K (1985) Relationship between the surface air temperature in Japan and sea water temperature in the western tropical Pacific during summer. Tenki 32:407–417 (in Japanese)
Kuroda K (2017) Longitude 137°E line initiated by Dr. Jotaro Matsuzawa of the Japan Meteorological Agency. Umi no Kenkyu (Oceanography in Japan) 26:251–258 (in Japanese with English abstract)
Lindstrom E, Lukas R, Fine R, Firing E, Godfrey S, Meyers G, Tsuchiya M (1987) The Western Equatorial Pacific Ocean Circulation Study. Nature 330:533–537
Lueker TJ, Dickson AG, Keeling CD (2000) Ocean pCO_2 calculated from dissolved inorganic carbon, alkalinity, and equations for K_1 and K_2: validation based on laboratory measurements of CO_2 in gas and seawater at equilibrium. Mar Chem 70:105–119
Lukas R (2001) Freshening of the upper thermocline in the North Pacific subtropical gyre associated with decadal changes of rainfall. Geophys Res Lett 28:3485–3488
Lukas R, Lindstrom E (1991) The mixed layer of the western equatorial Pacific ocean. J Geophys Res 96:3343–3358
Luo JJ, Yamagata T (2003) A model study on the 1988–89 warming event in the northern North Pacific. J Phys Oceanogr 33:1815–1828
Mantua NJ, Hare SR, Zhang Y, Wallace JM, Francis RC (1997) A Pacific interdecadal climate oscillation with impacts on salmon production. Bull Am Meteorol Soc 78:1069–1079
Mantyla AW, Reid JL (1983) Abyssal characteristics of the World Ocean waters. Deep Sea Res 30:805–833
Masuzawa J (1967) An oceanographic section from Japan to New Guinea at 137°E in January 1967. Oceanogr Mag 19:95–118
Masuzawa J (1968) Second cruise for CSK, Ryofu Maru, January to March 1968. Oceanogr Mag 20:173–185
Masuzawa J (1969) Subtropical mode water. Deep Sea Res 16:463–472
Masuzawa J (1970) Geostrophic flux of the North Equatorial current south of Japan. J Oceanogr Soc Jpn 26:61–64
Masuzawa J (1972) Water characteristics of the North Pacific central region. In: Stommel H, Yoshida K (eds) Kuroshio—its physical aspects. University Tokyo Press, Tokyo, pp 95–127
Masuzawa J (1978) Cooperative Study of the Kuroshio and Adjacent Regions (CSK) and I. Kaiyo Kagaku (Extra) 1:16–20 (in Japanese)
Masuzawa J, Nagasaka K (1975) The 137°E oceanographic section. J Mar Res 33(Suppl):109–116
Masuzawa J, Akiyama T, Kawarada Y, Sawara T (1970) Preliminary report of the Ryofu Maru Cruise Ry7001 in January–March 1970. Oceanogr Mag 22:1–25
Maximenko NA, Bang B, Sasaki H (2005) Observational evidence of alternating zonal jets in the world ocean. Geophys Res Lett 32:L12607. https://doi.org/10.1029/2005GL022728
McWilliams JC (2016) Submesoscale currents in the ocean. Proc R Soc A 472:20160117
Michaels AF, Knap AH (1996) Overview of the U.S. JGOFS Bermuda Atlantic Time-series Study and the Hydrostation S Program. Deep Sea Res II 43:157–198
Midorikawa T, Umeda T, Hiraishi N, Ogawa K, Nemoto K, Kudo N, Ishii M (2002) Estimation of seasonal net community production and air–sea CO_2 flux based on the carbon budget above the temperature minimum layer in the western subarctic North Pacific. Deep Sea Res I 49:339–362
Midorikawa T, Nemoto K, Kamiya H, Ishii M, Inoue HY (2005) Persistently strong oceanic CO_2 sink in the western subtropical North Pacific. Geophys Res Lett 32:L05612. https://doi.org/10.1029/2004GL021952
Midorikawa T, Ishii M, Nemoto K, Kamiya H, Nakadate A, Masuda S, Matsueda H, Nakano T, Inoue HY (2006) Interannual variability of winter oceanic CO_2 and air–sea CO_2 flux in the western North Pacific for 2 decades. J Geophys Res 111:C07S02. https://doi.org/10.1029/2005jc003095
Midorikawa T, Ishii M, Saito S, Sasano D, Kosugi N, Motoi T, Kamiya H, Nakadate A, Nemoto K, Inoue HY (2010) Decreasing pH trend estimated from 25-yr time series of carbonate parameters in the western North Pacific. Tellus Ser B 62:649–659
Midorikawa T, Ishii M, Sasano D, Kosugi N, Sugimoto H, Hiraishi N, Masuda S, Suzuki T, Takamura TR, Inoue HY (2011) Ocean acidification in the subtropical North Pacific estimated from accumulated carbonate data. Pap Meteorol Geophys 62:47–56
Midorikawa T, Ishii M, Kosugi N, Sasano D, Nakano T, Saito S, Sakamoto N, Nakano H, Inoue HY (2012) Recent deceleration of oceanic pCO_2 increase in the western North Pacific in winter. Geophys Res Lett 39:L12601. https://doi.org/10.1029/2012GL051665
Miyake Y, Sugimura Y (1969) Carbon dioxide in the surface water and the atmosphere in the Pacific, the Indian and the Antarctic Ocean areas. Rec Oceanogr Wks Jpn 10:23–28
Miyake Y, Sugimura Y, Saruhashi K (1974) The carbon dioxide content in the surface waters in the Pacific Ocean. Rec Oceanogr Wks Jpn 12:45–52
Murata AM, Fushimi K (1996) Temporal variations in atmospheric and oceanic CO_2 in the western North Pacific from 1990 to 1993: possible link to the 1991/92 ENSO event. J Metereol Soc Jpn 74:1–20
Murata AM, Kaneko I, Nemoto K, Fushimi K, Hirota M (1998) Spatial and temporal variations of surface seawater fCO_2 in the Kuroshio off Japan. Mar Chem 59:189–200
Nagai N, Tadokoro K, Kuroda K, Sugimoto T (2015) Latitudinal distribution of chaetognaths in winter along the 137°E meridian in the Philippine Sea. Plankton Benthos Res 10:141–153
Nagasaka K (1981) Long-term variation of sea water temperature. Tenki 28:553–556 (in Japanese)
Nagasaka K, Sawara T (1972) A preliminary report of the cruise of the R/V Ryofu-Maru in January–March 1971. Oceanogr Mag 24:25–38
Nakamura H (1996) A pycnostad on the bottom of the ventilated portion in the central subtropical North Pacific: its distribution and formation. J Oceanogr 52:171–188
Nakano T (2013) On the revisit of WOCE (World Ocean Circulation Experiment) one-time sections by the Japan Meteorological Agency. Weather Serv Bull 80(Sp):S111–S124 (in Japanese)
Nakano T (2016) Insights from a half-century of oceanographic observations. http://www.nippon.com/en/currents/d00309/. Accessed 30 Oct 2017
Nakano T, Kaneko I, Endoh M, Kamachi M (2005) Interannual and decadal variabilities of NPIW salinity minimum core observed along JMA's hydrographic repeat sections. J Oceanogr 61:681–697
Nakano T, Kaneko I, Soga T, Tsujino H, Yasuda T, Ishizaki H, Kamachi M (2007) Mid-depth freshening in the North Pacific subtropical gyre observed along the JMA repeat and WOCE hydrographic sections. Geophys Res Lett 34:L23608. https://doi.org/10.1029/2007GL031433
Nakano T, Kitamura T, Sugimoto S, Suga T, Kamachi M (2015) Long-term variations of North Pacific tropical water along the 137°E repeat hydrographic section. J Oceanogr 71:229–238
Nan F, Yu F, Wang R, Si G (2015) Ocean salinity changes in the northwest Pacific subtropical gyre: the quasi-decadal oscillation and the freshening trend. J Geophys Res 120:2179–2192
Nan'niti T (1960) Long-period fluctuations in the Kuroshio. Pap Meteorol Geophys 11:339–347

National Geophysical Data Center (2006) 2-minute gridded global relief data (ETOPO2) v2. National Geophysical Data Center, NOAA. https://doi.org/10.7289/v5j1012q. Accessed 9 Jan 2008

Niiler PP, Maximenko NA, Panteleev GG, Yamagata T, Olson DB (2003) Near-surface dynamical structure of the Kuroshio extension. J Geophys Res 108:3193. https://doi.org/10.1029/2002JC001461

Nishikawa H, Toyoda T, Masuda S, Ishikawa Y, Sasaki Y, Igarashi H, Sakai M, Seito M, Awaji T (2015) Wind-induced stock variation of the neon flying squid (*Ommastrephes bartramii*) winter-spring cohort in the subtropical North Pacific Ocean. Fish Oceanogr 24:229–241

Nitani H (1975) Variation of the Kuroshio south of Japan. J Oceanogr Soc Jpn 31:154–173

Nitta T, Yamada S (1989) Recent warming of tropical sea surface temperature and its relationship to the Northern Hemisphere circulation. J Meteorol Soc Jpn 67:375–382

Ogawa K, Takatani S (1998) Global Investigation of Pollution in the Marine Environment/Marine Pollution Monitoring Program (GIPME/MARPOLMoN). Weather Serv Bull 65(Sp):S139–S141 (in Japanese)

Oka E (2009) Seasonal and interannual variation of North Pacific subtropical mode water in 2003–2006. J Oceanogr 65:151–164

Oka E, Qiu B (2012) Progress of North Pacific mode water research in the past decade. J Oceanogr 68:5–20

Oka E, Suga T (2005) Differential formation and circulation of North Pacific central mode water. J Phys Oceanogr 35:1997–2011

Oka E, Qiu B, Takatani Y, Enyo K, Sasano D, Kosugi N, Ishii M, Nakano T, Suga T (2015) Decadal variability of subtropical mode water subduction and its impact on biogeochemistry. J Oceanogr 71:389–400

Oka E, Katsura S, Inoue H, Kojima A, Kitamoto M, Nakano T, Suga T (2017) Long-term change and variation of salinity in the western North Pacific subtropical gyre revealed by 50-year long observations along 137°E. J Oceanogr 73:479–490

Olsen A, Key RM, van Heuven S, Lauvset SK, Velo A, Lin X, Schirnick C, Kozyr A, Tanhua T, Hoppema M, Jutterström S, Steinfeldt R, Jeansson E, Ishii M, Pérez FF, Suzuki T (2016) The Global Ocean Data Analysis Project version 2 (GLODAPv2)—an internally consistent data product for the world ocean. Earth Syst Sci Data 8:297–323

Purkey SG, Johnson GC (2012) Global contraction of Antarctic bottom water between the 1980s and 2000s. J Clim 25:5830–5844

Qiu B (1999) Seasonal eddy field modulation of the North Pacific subtropical countercurrent: TOPEX/Poseidon observations and theory. J Phys Oceanogr 29:2471–2486

Qiu B, Chen S (2005) Variability of the Kuroshio extension jet, recirculation gyre, and mesoscale eddies on decadal time scales. J Phys Oceanogr 35:2090–2103

Qiu B, Chen S (2006) Decadal variability in the formation of the North Pacific subtropical mode water: oceanic versus atmospheric control. J Phys Oceanogr 36:1365–1380

Qiu B, Chen S (2010a) Interannual variability of the North Pacific subtropical countercurrent and its associated mesoscale eddy field. J Phys Oceanogr 40:213–225

Qiu B, Chen S (2010b) Interannual-to-decadal variability in the bifurcation of the north equatorial current off the Philippines. J Phys Oceanogr 40:2525–2538

Qiu B, Chen S (2012) Multidecadal sea level and gyre circulation variability in the northwestern tropical Pacific Ocean. J Phys Oceanogr 42:193–206

Qiu B, Chen S (2013) Concurrent decadal mesoscale eddy modulations in the western North Pacific subtropical gyre. J Phys Oceanogr 43:344–358

Qiu B, Joyce TM (1992) Interannual variability in the mid-and low latitude western North Pacific. J Phys Oceanogr 22:1062–1079

Qiu B, Chen S, Hacker P (2007) Effect of mesoscale eddies on subtropical mode water variability from the Kuroshio Extension System Study (KESS). J Phys Oceanogr 37:982–1000

Qiu B, Chen S, Carter GS (2012) Time-varying parametric subharmonic instability from repeat CTD surveys in the northwestern Pacific Ocean. J Geophys Res 117:C09012. https://doi.org/10.1029/2012JC007882

Qiu B, Rudnick DL, Chen S, Kashino Y (2013a) Quasi-stationary north equatorial undercurrent jets across the tropical North Pacific Ocean. Geophys Res Lett 40:2183–2187

Qiu B, Chen S, Sasaki H (2013b) Generation of the north equatorial undercurrent jets by triad baroclinic Rossby wave interactions. J Phys Oceanogr 43:2682–2698

Qiu B, Chen S, Schneider N, Taguchi B (2014a) A coupled decadal prediction of the dynamic state of the Kuroshio extension system. J Clim 27:1751–1764

Qiu B, Chen S, Klein P, Sasaki H, Sasai Y (2014b) Seasonal mesoscale and submesoscale eddy variability along the North Pacific subtropical countercurrent. J Phys Oceanogr 44:3079–3098

Qiu B, Nakano T, Chen S, Klein P (2017) Submesoscale transition from geostrophic flows to internal waves in the northwestern Pacific upper ocean. Nat Commun 8:14055. https://doi.org/10.1038/ncomms14055

Qu T, Lindstrom E (2002) A climatological interpretation of the circulation in the western South Pacific. J Phys Oceanogr 32:2492–2508

Rainville L, Jayne SR, Cronin MF (2014) Variations of the North Pacific subtropical mode water from direct observations. J Clim 27:2842–2860

Reid JL (1965) Intermediate waters of the Pacific Ocean. In: Johns Hopkins oceanography studies, vol 2. Johns Hopkins University Press, Baltimore, p 85

Reid JL (1973) The shallow salinity minima of the Pacific Ocean. Deep Sea Res 20:51–68

Ren L, Riser SC (2010) Observations of decadal time scale salinity changes in the subtropical thermocline of the North Pacific Ocean. Deep Sea Res II 57:1161–1170

Revelle R, Suess HE (1957) Carbon dioxide exchange between atmospheric and ocean and the question of an increase of atmospheric CO_2 during the past decades. Tellus 9:18–27

Rhein M, Rintoula S, Aoki S, Campos E, Chambers D, Feely R, Gulev S, Johnson G, Josey S, Kostianoy A, Mauritzen C, Roemmich D, Talley L, Wang F (2013) Observations: ocean. In: Stocker TF, Qin D, Plattner GK, Tignor M, Allen SK, Boschung J, Nauels A, Xia Y, Bex V, Midgley PM (eds) Climate change 2013: the physical science basis. Contribution of working group I to the fifth assessment report of the intergovernmental panel on climate change. Cambridge University Press, Cambridge

Roemmich D, Boebel O, Desaubies Y, Freeland H, King B, LeTraon PY, Molinari R, Owens WB, Riser S, Send U, Takeuchi K, Wijffels S (2001) Argo: the global array of profiling floats. In: Koblinsky CJ, Smith NR (eds) Observing the oceans in the 21st century. GODAE Project Office, Bureau of Meteorology, Melbourne, pp 248–258

Sagi T (1969a) The concentration of calcium and the calcium chlorosity ratio in the western North Pacific Ocean. Oceanogr Mag 21:61–66

Sagi T (1969b) The ammonia content in sea water in the western North Pacific Ocean. Oceanogr Mag 21:113–119

Sagi T (1970) On the distribution of nitrate nitrogen in the wesetern North Pacific Ocean. Oceanogr Mag 22:63–74

Sagi T, Yura T, Akiyama T (1974) The cadmium content in sea water in the adjacent regions of Japan and in the western North Pacific. Oceanogr Mag 25:101–110

Saiki M (1982) Relation between the geostrophic flux of the Kuroshio in the Eastern China Sea and its large-meander in the south of Japan. Oceanogr Mag 32:11–18
Saiki M (1987) Interannual variation of the subtropical gyre in the western North Pacific. Umi to Sora 63:113–125 (in Japanese with English abstract)
Saito S, Ishii M, Midorikawa T, Inoue HY (2008) Precise spectrophotometric measurement of seawater pH_T with an automated apparatus using a flow cell in a closed circuit. In: Tech report, vol 57. Meteorological Research Institute, Tsukuba
Sano A, Satoh N, Kubo N (1979) Floating particulate petroleum resideus, tar balls, in the western North Pacific. Oceanogr Mag 30:47–54
Sasano D, Ishii M, Midoriakwa T, Nakano T, Tokieda T, Uchida H (2011) Testing a new quick response sensor, "RINKO". Pap Meteorol Geophys 62:63–73
Sasano D, Takatani Y, Kosugi N, Nakano T, Midorikawa T, Ishii M (2015) Multidecadal trends of oxygen and their controlling factors in the western North Pacific. Global Biogeochem Cycles 29:935–956
Shibano R, Yamanaka Y, Okada N, Chuda T, Suzuki S, Niino H, Toratani M (2011) Responses of marine ecosystem to typhoon passages in the western subtropical North Pacific. Geophys Res Lett 38:L18608. https://doi.org/10.1029/2011GL048717
Shigehara K, Kimura K, Ohoyama J, Kubo N (1979) Fluorescing materials in marine environment and petroleum pollution: I. Analytical method and preliminary report of the result. Oceanogr Mag 30:61–74
Shuto K (1996) Internal variations of water temperature and salinity along the 137°E meridian. J Oceanogr 52:575–595
Smith WHF, Sandwell DT (1997) Global sea floor topography from satellite altimetry and ship depth soundings. Science 277:1956–1962
Soga T, Takatsuki Y, Hayashi K (2005) Variability of the North Pacific subtropical mode water along 137°E after mid-1990s. Weather Serv Bull 72(Sp):S131–S138 (in Japanese)
Sudo H (1986) Deep-water property variation below about 4000 m in the Shikoku Basin. La Mer 24:21–32
Suga T, Hanawa K (1990) The mixed layer climatology in the northwestern part of the North Pacific subtropical gyre and the formation area of subtropical mode water. J Mar Res 48:543–566
Suga T, Hanawa K (1995a) The subtropical mode water circulation in the North Pacific. J Phys Oceanogr 25:958–970
Suga T, Hanawa K (1995b) Interannual variations of North Pacific subtropical mode water in the 137°E section. J Phys Oceanogr 25:1012–1017
Suga T, Hanawa K, Toba Y (1989) Subtropical mode water in the 137°E section. J Phys Oceanogr 19:1605–1618
Suga T, Takei Y, Hanawa K (1997) Thermostad distribution in the North Pacific subtropical gyre: the central mode water and the subtropical mode water. J Phys Oceanogr 27:140–152
Suga T, Kato A, Hanawa K (2000) North Pacific tropical water: its climatology and temporal changes associated with the climate regime shift in the 1970s. Prog Oceanogr 47:223–256
Sugimoto S, Hanawa K (2011) Quasi-decadal modulations of North Pacific intermediate water area in the cross section along the 137°E meridian: impact of the Aleutian low activity. J Oceanogr 67:519–531
Sugimoto S, Hanawa K (2014) Influence of Kuroshio path variation south of Japan on formation of subtropical mode water. J Phys Oceanogr 44:1065–1077
Sugimoto S, Kako SI (2016) Decadal variation in winter mixed layer depth south of the Kuroshio extension and its influence on winter mixed layer temperature. J Clim 29:1237–1252
Sugimoto T, Tadokoro K (1998) Interdecadal variations of plankton biomass and physical environment in the North Pacific. Fish Oceanogr 7:289–299
Sugimoto S, Hanawa K, Narikiyo K, Fujimori M, Suga T (2010) Temporal variations of the Kuroshio transport and its relation to atmospheric variations. J Oceanogr 66:611–619
Suzuki T, Ishii M, Aoyama M, Christian JR, Enyo K, Kawano T, Key RM, Kosugi N, Kozyr A, Miller LA, Murata A, Nakano T, Ono T, Saino T, Sasaki K, Sasano D, Takatani Y, Wakita M, Sabine CL (2013) Pacifica data synthesis project. ORNL/CDIAC-159 NDP-092
Suzuoki T, Matsuzaki M (1983) Tar ball distribution and dynamics of surface waters in the western North Pacific. Oceanogr Mag 33:19–26
Suzuoki T, Shirakawa K (1979) Visual observation on the floating pollutants in open ocean. Oceanogr Mag 30:55–60
Sverdrup HU, Johnson MW, Fleming RH (1942) The oceans, their physics, chemistry, and general biology. Prentice-Hall, New York
Takahashi T (1961) Carbon dioxide in the atmosphere and in the Atlantic Ocean water. J Geophys Res 66:477–494
Takahashi T, Sutherland SC (2017) Global ocean surface water partial pressure of CO_2 data base: measurements performed during 1957–2016 (version 2016) NOAA/NCEI/OCADS NDP-088(V2016)
Takahashi T, Feely RA, Weiss RF, Wanninkhof RH, Chipman DW, Sutherland SC, Takahashi TT (1997) Global air–sea flux of CO_2. Proc Natl Acad Sci 94:8292–8299
Takatani S, Sagi T, Imai M (1986) Distributions of floating tars and petroleum hydrocarbons at the surface in the western North Pacific. Oceanogr Mag 36:33–42
Takatani S, Oikawa K, Kan O (1999) Long-term monitoring of background marine pollution (oil pollution) in the western North Pacific. Weather Serv Bull 66:S89–S96
Takatani Y, Sasano D, Nakano T, Midorikawa T, Ishii M (2012) Decrease of dissolved oxygen after the mid-1980s in the western North Pacific subtropical gyre along the 137E repeat section. Global Biogeochem Cycles 26:GB2013. https://doi.org/10.1029/2011gb004227
Takeuchi K (1986) Numerical study of the seasonal variations of the subtropical front and the subtropical countercurrent. J Phys Oceanogr 16:919–926
Talley LD (1993) Distribution and formation of North Pacific intermediate water. J Phys Oceanogr 23:517–537
Talley LD, Pickard GL, Emery WJ, Swift JH (2011) Descriptive physical oceanography: an introduction. Academic, New York, p 560
Tans PP, Fung IY, Takahashi T (1990) Observational constrains on the global atmospheric CO_2 budget. Science 247:1431–1438
Thomas LN, Tandon A, Mahadevan A (2008) Sub-mesoscale processes and dynamics. In: Hecht MW, Hasumi H (eds) Ocean modeling in an eddying regime, geophysical monograph series, vol 177. American Geophysical Union, Washington, DC, pp 17–38
Thorpe SA (1977) Turbulence and mixing in a Scottish Loch. Philos Trans R Soc A 286:125–181
Torii T, Yoshida Y, Hirayama Z (1959) Chemical studies on the nutrient matter in sea water between Cape Town and Lützow-Holm Bay, Antarctica. Antarct Rec 8:482–498
Toyoda T et al (2017) Interannual-decadal variability of wintertime mixed layer depths in the north pacific detected by an ensemble of ocean syntheses. Clim Dyn 49:891–907
Trenberth KE (1990) Recent observed interdecadal climate changes in the northern hemisphere. Bull Am Meteorol Soc 71:988–993
Trenberth KE, Hurrell JW (1994) Decadal atmosphereocean variations in the Pacific. Clim Dyn 9:303–319
Tseng Y-H et al (2016) North and equatorial Pacific Ocean circulation in the CORE-II hindcast simulations. Ocean Model 104:143–170

Tsuchiya M (1968) Upper waters of the intertropical Pacific Ocean. In: Johns Hopkins oceanography studies, vol 4. Johns Hopkins University Press, Baltimore, p 50

Tsuchiya M (1975) Subsurface countercurrents in the eastern equatorial Pacific Ocean. J Mar Res 33(Suppl):S145–S175

Tsuchiya M (1991) Flow path of the Antarctic intermediate water in the western equatorial South Pacific Ocean. Deep Sea Res 38(Suppl):S273–S279

Tsuchiya M, Lukas R, Fine RA, Firing E, Lindstrom E (1989) Source waters of the Pacific equatorial undercurrent. Prog Oceanogr 23:101–147

Tsukamoto K (1992) Discovery of the spawning area for Japanese eel. Nature 356:789–791

Tsukamoto K (2006) Spawning of eels near seamount. Nature 439:929

Uchida H, Johnson GC, McTaggart KE (2011) CTD oxygen sensor calibration procedures. In: The GO-SHIP repeat hydrography manual: a collection of expert reports and guidelines, IOCCP report 14, ICPO publication series 134 Ver.1

Uda M, Hasunuma K (1969) The eastward subtropical countercurrent in the western North Pacific Ocean. J Oceanogr Soc Jpn 25:201–210

Uehara K, Taira K (1990) Deep hydrographic structure along 12°N and 13°N in the Philippine Sea. J Oceanogr 46:167–176

Usui N, Tsujino H, Nakano H, Matsumoto S (2013) Long-term variability of the Kuroshio path south of Japan. J Oceanogr 69:647–670

Wada A, Midorikawa T, Ishii M, Motoi T (2011) Carbon system changes in the East China Sea induced by Typhoons Tina and Winnie in 1997. J Geophys Res 116:C07014. https://doi.org/10.1029/2010JC006701

Watanabe YW, Ishida H, Nakano T, Nagai N (2005) Spatiotemporal decreases of nutrients and chlorophyll-*a* in the surface mixed layer of the western North Pacific from 1971 to 2000. J Oceanogr 61:1011–1016

White WB (1995) Design of a global observing system for gyre-scale upper ocean temperature variability. Prog Oceanogr 36:169–217

White WB, Hasunuma K, Solomon H (1978) Large-scale seasonal, secular variability of the subtropical front in the western North Pacific from 1954 to 1974. J Geophys Res 83:4531–4544

White WB, Meyers G, Hasunuma K (1982) Space/time statistics of short-term climatic variability in the western North Pacific. J Geophys Res 87:1979–1989

Whitney FA, Freeland HJ (1999) Variability in upper-ocean water properties in the NE Pacific Ocean. Deep Sea Res II 46:2351–2370

Wong APS, Bindoff NL, Church JA (1999) Large-scale freshening of intermediate waters in the Pacific and Indian Oceans. Nature 400:440–443

Wong APS, Bindoff NL, Church JA (2001) Freshwater and heat changes in the north and south Pacific Oceans between the 1960s and 1985–94. J Clim 14:1613–1633

Wunsch C, Ferrari R (2004) Vertical mixing, energy and the general circulation of the oceans. Ann Rev Fluid Mech 36:281–314

Wyrtki K (1961) Physical oceanography of the southeast Asian waters. In: NAGA report 2, Scripps Institute of Oceanographhy, University of California, San Diego, p 195

Wyrtki K, Kilonsky B (1984) Mean water and current structure during the Hawaii-to-Tahiti shuttle experiment. J Phys Oceanogr 14:242–254

Yara Y, Vogt M, Fujii M, Yamano H, Hauri C, Steinacher M, Gruber N, Yamanaka Y (2012) Ocean acidification limits temperature-induced poleward expansion of coral habitats around Japan. Biogeosciences 9:4955–4968

Yasuda I (2004) North Pacific intermediate water: progress in SAGE (SubArctic Gyre Experiment) and related projects. J Oceanogr 60:385–395

Yasunari T (1990) Impact of Indian monsoon on the coupled atmosphere/ocean system in the tropical Pacific. Meteorol Atmos Phys 44:29–41

Yoon JH, Yasuda I (1987) Dynamics of the Kuroshio large meander: two-layer model. J Phys Oceanogr 17:66–81

Yuan X, Talley LD (1992) Shallow salinity minima in the North Pacific. J Phys Oceanogr 22:1302–1316

Zenimoto K, Kitagawa T, Miyazaki S, Sasai Y, Sasaki H, Kimura S (2009) The effects of seasonal and interannual variability of oceanic structure in the western Pacific North equatorial current on larval transport of the Japanese eel *Anguilla japonica*. J Fish Biol 74:1878–1890

Zhai F, Hu D, Qu T (2013) Decadal variations of the North equatorial current in the Pacific at 137°E. J Geophys Res 118:4989–5006